Hydrothermal Alteration in Research Drill Hole Y–6, Upper Firehole River, Yellowstone National Park, Wyoming

U.S. GEOLOGICAL SURVEY PROFESSIONAL PAPER 1054–B

Hydrothermal Alteration in Research Drill Hole Y–6, Upper Firehole River, Yellowstone National Park, Wyoming

By KEITH E. BARGAR *and* MELVIN H. BEESON

HYDROTHERMAL STUDIES IN YELLOWSTONE NATIONAL PARK, WYOMING

U.S. GEOLOGICAL SURVEY PROFESSIONAL PAPER 1054–B

UNITED STATES GOVERNMENT PRINTING OFFICE, WASHINGTON : 1984

DEPARTMENT OF THE INTERIOR

WILLIAM P. CLARK, ***Secretary***

U.S. GEOLOGICAL SURVEY

Dallas L. Peck, ***Director***

Library of Congress Cataloging in Publication Data

Bargar, Keith E.
Hydrothermal alteration in research drill hole Y-6, Upper Firehole River, Yellowstone National Park, Wyoming.

(Hydrothermal studies in Yellowstone National Park, Wyoming) (Geological Survey professional paper 1054-B)
Bibliography: p. B22-B24 .
Supt. of Docs. no.: I 19.16:1054-B
1. Hydrothermal deposits—Wyoming—Firehole River Valley. 2. Borings—Wyoming—Firehole River Valley. I. Beeson, Melvin H. II. Title. III. Series. IV. Series: U.S. Geological Survey professional paper 1054-B.

QE461.B294 1984 552 84-600005

For sale by the Distribution Branch, Text Products Section,
U.S. Geological Survey, 604 South Pickett St., Alexandria, VA 22304

CONTENTS

ILLUSTRATIONS

TABLES

HYDROTHERMAL ALTERATION IN RESEARCH DRILL HOLE Y–6, UPPER FIREHOLE RIVER, YELLOWSTONE NATIONAL PARK, WYOMING

By KEITH E. BARGAR and MELVIN H. BEESON

ABSTRACT

Y–6, a U.S. Geological Survey research diamond-drill hole in the upper Firehole River area of Yellowstone National Park, Wyoming, penetrated a surface covering of Pinedale glacial sediments and about 130 m of the Scaup Lake flow of the Upper Basin Member of the Pleistocene Plateau Rhyolite. The groundmass of the rhyolite flow has been extensively devitrified to α-cristobalite and sanidine, and vapor-phase zones contain granophyric quartz, alkali feldspar, and some magnetite and tridymite. Abundant fractures, possibly related to Mallard Lake resurgent doming, are mostly filled (self-sealed) by hydrothermal minerals, dominantly chalcedony. Other hydrothermal minerals deposited along fractures and in cavities in the drill core include quartz, zeolite minerals (clinoptilolite, dachiardite, intermediate heulandite, and mordenite), iron and manganese carbonate minerals (Mn-calcite, Ca- and Fe-rhodochrosite, rhodochrosite, and siderite), apatite, iron sulfides (pyrite and marcasite), iron oxides and hydroxides (goethite and hematite), clay minerals (iron-rich chlorite, kaolinite, mixed-layer illite-smectite and smectite) and a 10-A mica. There is some indication that the waters flowing through the Y–6 drill core previously were warmer and cooled to the present temperatures due to self-sealing coupled with the downward percolation of cold meteoric water. Adularia and bladed calcite in open-space deposits may have formed at an earlier time from boiling of the thermal water that led to a loss of CO_2 and an increase in pH. Fluorite, which was deposited later than calcite, probably formed due to decreasing solubility as the temperature decreased. Fluid inclusion studies of four samples show a wide range of homogenization temperatures that are significantly warmer than the measured temperature curve.

INTRODUCTION

Research diamond-drill hole Y–6 is one of the 13 holes drilled by the U.S. Geological Survey at selected sites in hot-spring and geyser areas of Yellowstone National Park, Wyoming (fig. 1). The holes were drilled during 1967 and 1968 in order to obtain detailed chemical and physical data on the shallow part of a high-temperature geothermal system. Y–6 is located about 0.5 km west of Lone Star Geyser and is 38 m northeast of and 2.1 m above the level of the upper Firehole River (at an elevation of 2,329 m) (White and others, 1975).

The drilling of Y–6, using water as the circulating fluid, began August 17, 1967, and ended September 1, 1967, at a depth of 152.3 m. Core recovery (by wireline method) was only about 1 percent in the poorly consolidated sands and gravels of the upper 21.2 m but averaged about 97.8 percent throughout the remainder of the drill hole.

The drill core was logged at the drill site by J. M. Mattinson, L. J. P. Muffler, and D. E. White. Approximately 270 pieces of the core that are representative of coring intervals (usually 1.5 or 3.0 m thick) or that contain secondary mineralization in veins, vugs, or fractures were selected for detailed

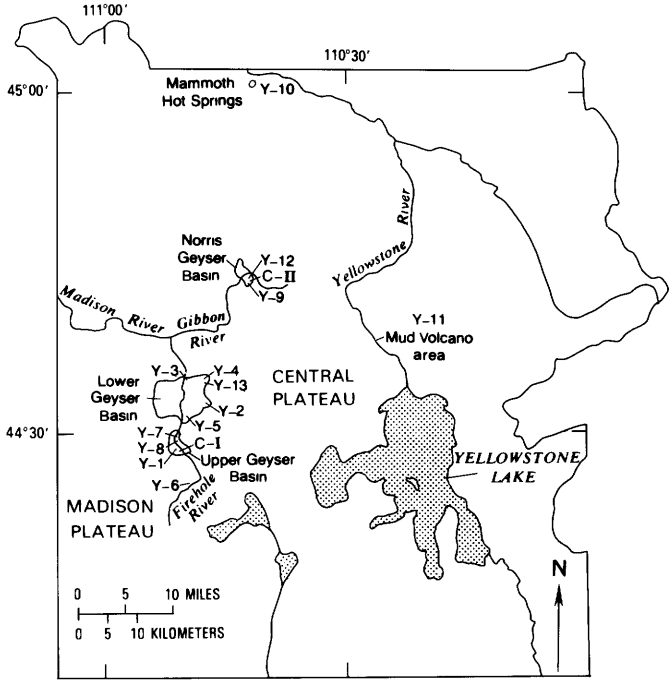

FIGURE 1.—Index map of Yellowstone National Park showing location of Y–6 and other research drill holes. Drill holes C–I and C–II drilled by the Carnegie Institution of Washington in 1929 (Fenner, 1936). Drill holes Y–1 through Y–13 drilled by U.S. Geological Survey.

laboratory study. This selected core was sytematically studied by petrographic, X-ray diffraction, electon microprobe, and scanning electron microscope (SEM) methods. Whole-rock chemical analyses by rapid rock method, semiquantitative spectrographic analyses, and bulk and powder density measurements were obtained for seven selected core samples.

White and others (1975) discussed the physical results of the 13 research drill holes. They reported a near-bottom fluid pressure of 1,570 kPa for drill hole Y–6. Temperature data shown in figure 2 were measured during drilling. Low surface temperatures are attributed to the flow of cold meteoric water through the unconsolidated sand and gravel surficial deposits. The temperature profile deeper in the drill hole is nearly parallel to the reference boiling point curve but is consistently lower. White and others (1975) and White (1978) indicated that Y–6 is probably on the border of a convection system and that the recorded temperatures lower than but parallel to the reference boiling curve may be due to lateral movement and conductive cooling of thermal water away from the main vertical channels of flow. The maximum temperature recorded was 180.8°C at a depth of 152 m; however, Fournier and Truesdell (1970) indicated that the aquifer temperature, based on the silica content (245 mg/L) of a nearby hot spring, may be as high as 193°C. The chemical composition of a near-neutral water subsequently analyzed (consisting predominantly of Na^+, Cl^-, HCO_3, and SiO_2) from the Y–6 drill hole (table 1) also suggests a higher aquifer temperature.

Chemical compositions of the Y–6 drill-hole water and of nearby hot-spring waters (Thompson and others, 1975; Thompson and Yadav, 1979) are similar to Upper Geyser Basin hot-spring water (White and others, 1975). White and others (1975) postulated that the Lone Star-upper Firehole River area lies within the Upper Geyser Basin hydrothermal convective system; the drilling data are consistent with this hypothesis but do not provide confirmation.

TABLE 1.—*Chemical composition (in milligrams per liter), pH, and calculated geothermometers (in degrees Celsius) of thermal water from Y–6 drill hole*

[Analyst: J. M. Thompson, U.S. Geological Survey, Geothermometers calculated from formulas presented in table 4.1 of Fournier (1981)]

SiO_2	244
Ca	4.56
Mg	0.075
Na	315
K	22.3
Li	1.77
HCO_3	202
SO_4	24
Cl	355
F	13.1
B	3.9
Total	1185.705
pH (field)	6.42
Quartz (conductive)	194
Quartz (adiabatic)	180
Chalcedony	175
Na/K (Fournier)	189
Na/K (Truesdell)	153
Na-K-Ca	186

ACKNOWLEDGMENTS

The authors were assisted by R. L. Oscarson in obtaining SEM micrographs, J. R. Boden in electron microprobe studies, and C. N. Bargar in X-ray diffraction studies. We thank R. O. Fournier, T. E. C. Keith, M. J. Reed, and D. E. White for their critical reviews and helpful discussion of the manuscript. Special thanks also go to J. M. Thompson for permitting the use of his water-chemistry data and for informative discussion of the water chemistry of the drill hole.

STRATIGRAPHY

GLACIAL SEDIMENTS

The upper 21.2 m of the Y–6 drill core is composed of poorly consolidated fluvial outwash material (fig. 2; Christiansen and Blank, 1974; Waldrop, 1975) that probably was deposited during the latter part of the Pinedale Glaciation (≥45,000 to 14,000 years ago) (Pierce and others, 1976). No core was recovered from this interval. Three samples of core-bit cuttings consist of (1) subrounded to rounded, fine sand to granule-sized particles of black obsidian, quartz, and rhyolite, (2) medium to very coarse pebbles of rhyolite, and (3) weakly cemented fine-grained sandstone and siltstone.

VOLCANIC ROCKS

From 21.2 m to the bottom of the drill hole at 152.3 m, the core penetrated the Scaup Lake flow of the Upper Basin Member of the Pleistocene Plateau Rhyolite (Christiansen and Blank, 1974; White and others, 1975). The Scaup Lake flow has a K-Ar date of approximately 265,000 years B.P. (J. D. Obradovich and R. L. Christiansen, unpub. data, 1973).

The upper part of the Scaup Lake flow (21.9 to 30.9 m) in core Y–6 consists of green to greenish-

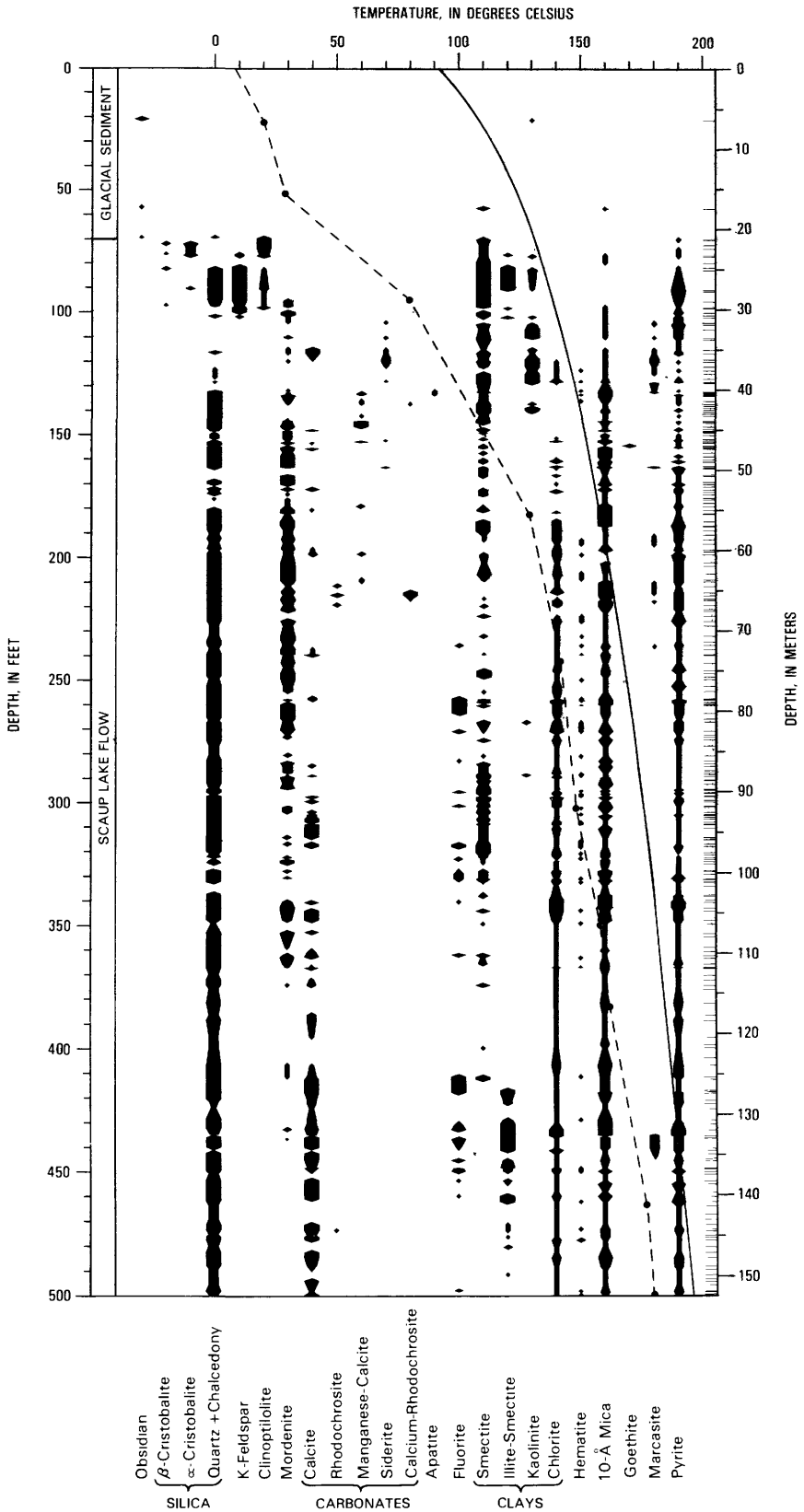

FIGURE 2.—Plot showing depth distribution of unaltered obsidian and hydrothermal alteration minerals in drill core from Y-6. Left column shows a stratigraphic section of rock units penetrated by the drill hole. Horizontal lines at right indicate distribution of samples studied. Width of mineral columns provides an estimate of relative abundance based on microscopic observation and X-ray diffraction analyses. Vertical continuity in mineral presence between samples is assumed except where a mineral abundance becomes zero, in which case the zero point is arbitrarily placed 0.3 m from last occurrence of the mineral. Dashed curve connects bottom-hole temperature measurements obtained as drilling progressed. Solid curve shows reference boiling temperature for pure water assuming a surface altitude of about 2,329 m and a water table at the surface. Temperature data from White and others (1975).

gray pumiceous and vitrophyric rhyolite flow breccia. A greenish to grayish rhyolite flow between 31.6 m and 45.6 m contains abundant lithophysal cavities. Below 45.6 m scattered lithophysal cavities are present in the rhyolite flow, but large irregular cavities and elongate vesicles that are oriented parallel to flow banding are more common. Much of the groundmass in the Scaup Lake flow is microspherulitic, and α-cristobalite, formed by devitrification, was identified by X-ray diffraction from 21.3 to 35.0 m, 40.2 to 41.4 m, 43.9 to 56.9 m, and in scattered samples down to 123.8 m. The microspherulitic texture persists in thin sections to near the bottom of the hole (151 m), but whole-rock X-ray diffraction analyses show only quartz and K-feldspar, suggesting recrystallization of the α-cristobalite. Phenocryst mineralogy throughout the Scaup Lake flow is nearly uniform and consists mostly of quartz and sanidine, minor plagioclase, and partly to completely altered mafic crystals (magnetite and pyroxene).

Lithophysal cavities and vesicles from 40.2 to 40.8 m, 43.9 to 47.8 m, and 80.2 to 97.4 m contain large (up to approximately 1 cm in length and 3 mm in width) euhedral quartz crystals. A few of the pyramidal or dipyramidal quartz crystals are coated by later vapor-phase alkali feldspar. Similar large prismatic quartz crystals found in Y–5 drill core were interpreted as being granophyric deposits in miarolitic cavities by Keith and Muffler (1978).

Most cavities and a few large vugs above 54.0 m in the rhyolite flow are lined by vapor-phase sanidine crystals that are usually coated by minute quartz crystals. Below 54.0 m, vapor-phase alkali feldspar crystals appear to be hydrothermally replaced by quartz similar to that described by Keith and Muffler (1978) in drill core Y–5. Tiny, quartz-coated, opaque grains (that are attracted to a magnet) were deposited later than vapor-phase alkali feldspar, and they may be of vapor-phase origin, as were the octahedral magnetite grains found in association with vapor-phase sanidine and tridymite in drill core Y–5. Widely separated X-ray diffractograms of whole-rock samples show the presence of vapor-phase tridymite between 45.2 and 98.3 m.

The Y–6 drill core is highly fractured, and a few pieces of core contain hydrothermal chalcedony fracture fillings and brecciation similar to that described for drill core Y–5 which Keith and Muffler (1978) attributed to tension associated with magmatic resurgence of the Mallard Lake dome. The southern margin of the Mallard Lake resurgent dome is located only about 2 km from the site of the Y–6 drill hole (Eaton and others, 1975; Christiansen, 1979) and could be responsible for much of the fracturing observed in this drill core.

HYDROTHERMAL ALTERATION

Figure 2 shows the distribution of hydrothermal minerals with depth in the Y–6 drill core. Most of the glass in the Scaup Lake flow, as indicated by the widespread microspherulitic texture, was devitrified. Later hydrothermal alteration minerals are mostly associated with fractures, lithophysal cavities, and other vugs that are usually lined or completely filled by at least one of the more than 20 hydrothermal minerals listed in figure 2. The earliest deposited hydrothermal minerals characteristically are silica and iron-rich minerals (red chalcedony, hematite, goethite, pyrite, marcasite, and quartz), and these are followed by clay minerals (smectite, illite-smectite, and kaolinite), apatite, carbonate minerals, fluorite, mordenite, chlorite, and later generations of smectite, quartz, and pyrite. Hydrothermal 10–A mica usually was found in combination with chlorite. Paragenesis of the remaining hydrothermal zeolite minerals (clinoptilolite, intermediate heulandite, and dachiardite), adularia, and silica minerals (β-cristobalite, and α-cristobalite) was not determined.

SILICA MINERALS

α- and β-CRISTOBALITE

β-cristobalite[1] was identified by X-ray diffraction in open-space deposits of a few scattered pieces of core between 21.9 and 44.0 m. At 21.9 m, hard, milky white β-cristobalite partly fills a cavity. The β-cristobalite has a horizontal (perpendicular to drill core that is assumed to be vertical) upper surface that is coated by later white, powdery α-cristobalite. β-cristobalite in vein or fracture fillings at 29.7 m is associated with white fibrous mordenite. Open-space deposits at 25.1 and 44.0 m consist of clear to white beaded to colloform chalcedony and minor β-cristobalite that was deposited earlier than clear quartz crystals at 25.1 m and later than white bladed calcite at 44.0 m.

[1] β-cristobalite has a broad major X-ray peak between 4.07 and 4.11 A and a single minor peak near 2.5 A; α-cristobalite has a sharp peak between 4.04 and 4.07 A along with several minor peaks.

When viewed in refractive-index oils under a petrographic microscope, mineral fragments from these two deposits appear to be composed of clear chalcedony (IR~1.53) that is interlayered with thin, very weakly birefringent bands of β-cristobalite.

White to gray, powdery or clayey fracture fillings and milky white dense to powdery horizontal cavity fillings from 21.9 to 27.6 m were identified as hydrothermal α-cristobalite by X-ray diffraction (see footnote 1). SEM studies of open-space α-cristobalite fillings at 21.9 m indicate that the mineral was deposited as aggregates of very fine grained bladed crystals similar to those described by Murata and Larson (1975) for poorly ordered β-cristobalite rather than the spiny or nubby crystals they illustrate for examples of better ordered α-cristobalite. This Y–6 sample has a major sharp X-ray peak at 4.07 A, a minor peak at 2.49 A, and poorly defined peaks at 2.85 and 3.14 A and was identified as α-cristobalite on the basis of the X-ray diffraction data; however, it appears to be transitional between well-ordered α-cristobalite and poorly ordered β-cristobalite.

QUARTZ AND CHALCEDONY

Chalcedony is present throughout much of the Scaup Lake flow as red, green, or white cryptocrystalline fracture and vug fillings. Red chalcedony (with associated hematite, determined by X-ray analyses) is the most abundant hydrothermal mineral found in the Y–6 drill core. Red chalcedony is the earliest hydrothermal mineral deposited on most fractures and occurs as horizontal (perpendicular to drill core) fillings in the bottoms of many cavities. Clear, colloform open-space fillings of banded chalcedony and β-cristobalite occur at 25.1 and 44.0 m. White to frosted colloform chalcedony "dripstone" stalactites, deposited later than red chalcedony, coat most of a 60°–dip fracture at 66.1 m. The upper right-hand corner of the fracture has similar-appearing "dripstone" stalactite deposits that are composed of tiny, clear quartz crystals rather than chalcedony.

Hydrothermal quartz is sparse to scattered in the upper 54.9 m of the drill core. Below that depth, clear quartz crystals (usually less than about 4 mm in length) line most fractures and cavities. Crystalline quartz appears to be an early hydrothermal mineral and probably was deposited shortly following deposition of closely associated chalcedony. However, several pieces of core contain examples of a later generation of quartz crystals that coat mordenite fibers and are pseudomorphous after bladed calcite (fig. 3). The top layer of a thinly banded, horizontal, white to green cryptocrystalline chalcedony cavity deposit at 41.8 m appears granular under the binocular microscope and may be similar to saccharoidal quartz described by Keith and Muffler (1978) from cavity fillings in drill core Y–5. SEM studies show that such granular cavity deposits in drill core Y–6 are composed of loosely packed, subhedral, dipyramidal quartz grains (fig. 4).

Murata and Norman (1976) proposed a method for numerically indexing the degree of crystallinity for quartz that is based on resolution of the d(212) X-ray peak at about 1.38 A. They found that clear, euhedral quartz crystals consistently have a nearly perfect crystallinity (index near 10 on a scale of 1 to 10) and that most chert or chalcedony samples have very low crystallinity except for strongly metamorphosed samples. Crystallinity indices, using Murata and Norman's method, were determined for 15 quartz and chalcedony samples that were fairly well distributed between 25.1 and 103.3 m in Y–6 drill core. One of the samples was a clear euhedral quartz crystal that is very well crystallized and has a maximum index (10). Other samples analyzed included cryptocrystalline chalcedony, granular quartz (like fig. 4), crystalline quartz replacing calcite (like fig. 3), clear colloform chalcedony, and crystalline quartz coating vapor-phase sanidine. All of these analyzed samples have moderate indices of crystallinity that range

FIGURE 3.—Scanning electron micrograph showing aggregates of tiny quartz crystals that are pseudomorphous after bladed calcite and partly coat fibrous mordenite.

between about 3 and 7 but do not show a correlation of increasing crystallinity index with increasing observed crystallinity from chalcedony to quartz.

POTASSIUM FELDSPAR

Adularia (hydrothermal potassium feldspar) (fig. 5) in drill core Y–6 was identified as cavity and fracture fillings between 23.2 and 30.9 m, a zone where temperatures measured during drilling were about 60° to 80°C (see fig. 2). Adularia is associated with chalcedony, clinoptilolite, smectite, illite-smectite, and kaolinite in X-ray diffractograms and was observed in SEM studies to be deposited later than hydrothermal ∝-cristobalite and earlier than quartz, mordenite, and some clay. Chemical analyses of this monoclinic potassium feldspar (table 2) indicate that it is nearly a pure potassium end member. In figure 6 the composition of adularia is shown in comparison with magmatic plagioclase and sanidine phenocrysts from the Y–6 drill core.

Browne and Ellis (1970) identified three methods of hydrothermal potassium feldspar formation in the Ohaki-Broadlands geothermal area of New Zealand: (1) Replacement of magmatic plagioclase phenocrysts, (2) introduction of significant potassium, or (3) depletion of carbon dioxide leading to an increase in pH during boiling of the geothermal water. Browne (1970) and Browne and Ellis (1970) indicated that adularia commonly forms at temperatures above 220°C and is characteristic of the hotter upflow channels but noted a single occurrence at 75°C.

Hydrothermal potassium feldspar previously has been identified in Yellowstone drill cores Y–1 (Honda and Muffler, 1970), C–I (Fenner, 1936), Y–8 (Keith and others, 1978b), Y–13 (Keith and others, 1978a), and Y–2 (Bargar and Beeson, 1981). Temperatures, measured during drilling by White and others (1975), at the shallowest occurrence of adularia in these drill holes are: 134.1°C (Y–1), 110°C (Y–8), 70°C (Y–13), and 150°C (Y–2). In drill hole C–I, the temperature was not measured at the shallowest adularia occurrence, but interpolation between data points suggests that the temperature was about 50°C.

Hydrothermal adularia and albite occur in leached plagioclase phenocrysts in drill core Y–13, and hydrothermal potassium feldspar overgrowths of clastic sanidine and plagioclase were found in drill core Y–8 by Keith and others (1978b). These authors indicated that hydrothermal potassium feldspar in Y–8 may have formed during conversion of clinoptilolite to analcime. Keith and others also attributed the abundant adularia in drill cores Y–13 and C–I to boiling of the thermal water. In Y–2 the origin of adularia is uncertain.

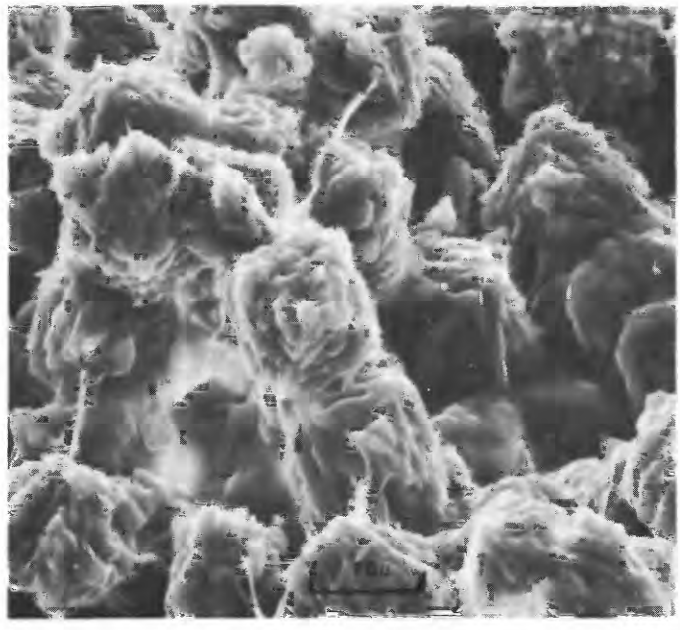

FIGURE 4.—Scanning electron micrograph showing granular cavity filling from core Y–6 at 40.3 m. Subhedral dipyramidal quartz grains are coated by smectite (identified by X-ray diffraction).

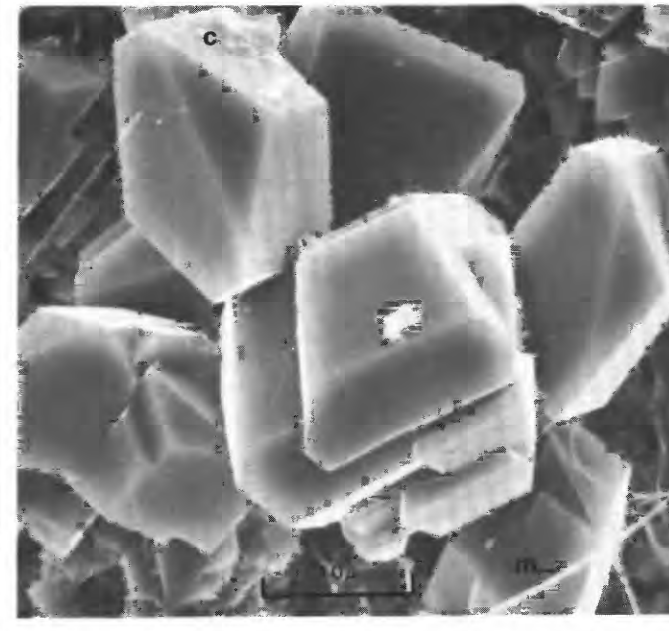

FIGURE 5.—Scanning electron micrograph showing euhedral adularia crystals that line a cavity in core Y–6 at 24.7 m. Small patches of clay (c) (smectite or illite-smectite) and fibrous mordenite (m) were deposited later than the adularia.

TABLE 2.—*Microprobe analyses of feldspars from Y–6 drill core*
[Analyst: J. R. Boden, U. S. Geological Survey]

Sample No.[1]	21.3	21.3	21.3	22.4	22.4	25.1	25.1	25.1	29.7	29.7	31.6
Mineral[2]–	S	S	P	S	P	A	P	A	P	S	S
					Weight percent						
SiO_2-----	64.90	64.33	63.32	64.90	62.12	63.46	62.24	65.59	62.79	64.38	64.25
Al_2O_3----	20.44	20.34	23.23	19.72	23.32	18.26	22.39	18.50	23.08	20.20	20.75
CaO------	.73	.76	4.61	.81	4.80	.28	3.90	.42	4.23	.66	.74
Na_2O-----	4.30	4.20	8.27	4.27	8.38	.14	7.71	.55	8.23	4.80	4.36
K_2O------	10.19	9.93	1.64	9.30	1.54	13.86	2.52	14.20	2.41	8.93	8.29
Total-	100.56	99.56	101.07	99.00	100.16	96.00	98.76	99.26	100.74	98.97	98.38
					Number of atoms on the basis of 32 oxygens						
Si-------	11.708	11.706	11.150	11.827	11.060	12.053	11.232	12.067	11.136	11.738	11.716
Al-------	4.346	4.363	4.823	4.236	4.894	4.088	4.762	4.012	4.825	4.340	4.459
Ca-------	.140	.148	.869	.158	.916	.057	.754	.083	.804	.129	.144
Na-------	1.504	1.482	2.824	1.507	2.894	.051	2.698	.198	2.829	1.696	1.542
K--------	2.346	2.306	.369	2.162	.350	3.358	.580	3.334	.546	2.077	1.929

[1] Sample numbers correspond to depth in meters.
[2] S = sanidine, P = plagioclase, A = adularia.

Adularia occurs in two zones in Y–2 drill core; the measured temperature of the lower zone exceeds the reference boiling point curve (see fig. 2 in Bargar and Beeson, 1981), and the temperature range for the upper adularia zone is close to the reference boiling curve and would need to have been only a few degrees warmer in the past in order to account for the formation of adularia by this method.

In drill core Y–6, adularia did not form by replacement of magmatic plagioclase, and the presence of clinoptilolite (and lack of analcime) in the hydrothermal potassium feldspar zone indicates that adularia probably did not form by release of potassium, and aluminum, at the expense of clinoptilolite. The explanation, favored for deposition of hydrothermal potassium feldspar in the upper part of the Scaup Lake flow in drill core Y–6 and for the existence of near-surface adularia in drill core Y–13, also at a temperature of about 70°C (T. E. C. Keith, oral commun., 1981), is that adularia is an indicator of a previously higher near-surface temperature and formed as a result of the loss of CO_2 and an increase in pH and the K/H ratio due to boiling of the thermal water (Keith and others, 1978b). White and others (1975) attributed the present low near-surface temperature in drill hole Y–6 to an influx of cold meteoric water that percolates down through the mantle of unconsolidated glacial sediments.

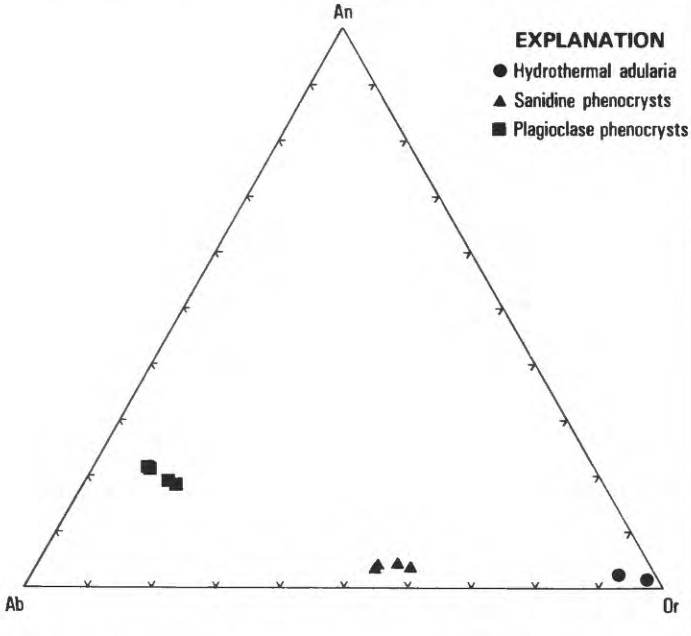

FIGURE 6.—An-Ab-Or ternary diagram of feldspar minerals from Y–6 drill core. Data from table 2.

ZEOLITE MINERALS

HEULANDITE-GROUP MINERALS

Euhedral, tabular or "tombstone" crystals of heulandite-group minerals (fig. 7) line cavities between 17.4 and 29.8 m in drill core Y–6 in association with hydrothermal ∝-cristobalite, adularia, smectite, and mordenite. X-ray diffraction patterns of heulandite-group minerals (heulandite, intermediate heulandite, and clinoptilolite) are virtually identical and a check of the thermal stability of these minerals by overnight heating at

450°C (Mumpton, 1960) or chemical analysis is required for identification of the individual minerals. Most of the heated samples from core Y–6 showed no change in intensity or displacement of the 020 X-ray peak at about 8.9 A and are thus classified as clinoptilolite. A single sample from 17.4 m showed considerable decrease in intensity and displacement of the 020 peak to about 8.3 A following the heat treatment. The structure was completely destroyed by heating at 550°C, and the mineral was reported as heulandite (Bargar and others, 1981).

Electron microprobe chemical analyses (table 3) of the 17.4–m sample show silicon/aluminum atomic ratios (Si/Al) of 3.34 to 3.82, sum of coefficients for divalent cations (SD) (only Ca in Y–6) of 2.08 to 2.34, and divalent/monovalent cation atomic ratios (SD/SM) (Ca/(Na + K)) of 1.16 to 2.15. According to heulandite-group mineral classification schemes that are based upon these parameters (discussed by Alietti, 1972; Boles, 1972; Alietti and others, 1977), the mineral from 17.4 m appears to be an intermediate heulandite although there is some overlap of Si/Al and SD/SM values with heulandite. Hawkins (1974) divided the heulandite-group minerals into two main groupings (group I, heulandite; group II, clinoptilolite) and five subgroupings (A–E), using multivariate statistical methods, according to discriminant functions based on CaO content. Using Hawkins' classification, the analyses for the sample from

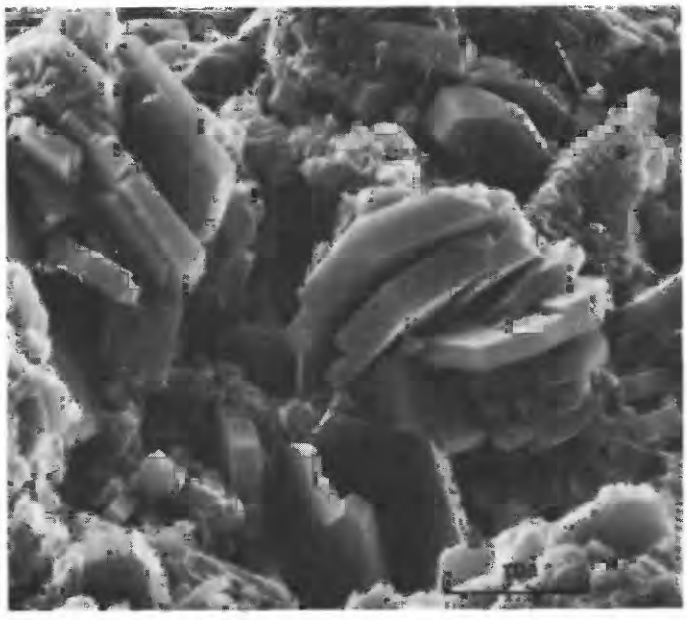

FIGURE 7.—Scanning electron micrograph showing tabular intermediate heulandite crystals and later boxwork smectite (s) and fibrous mordenite (m) (after Bargar and others, 1981).

TABLE 3.—*Microprobe analyses of heulandite-group minerals from Y–6 drill core*

[Sample numbers correspond to depth in meters]

Sample	Y6-17.41						Y6-21.3[2,4]				Y6-22.42[,4]					
	Weight percent															
SiO_2	62.54	62.72[5]	61.53[3]	59.38[3]	59.77[3]	60.00[3,5]	61.44[3,5]	60.26	71.08	68.61	70.97	68.33	68.69	58.73	61.12	62.15	64.62	67.04
Al_2O_3	13.89	14.08	15.61	14.90	14.74	15.00	15.22	11.51	14.11	14.63	14.59	13.68	14.43	12.60	12.79	12.95	13.69	14.26
Fe_2O_3	--	--	.45	.45	.60	.82	.44	.00	.00	.00	.00	.00	.00	.00	.00	.00	.00	.00
CaO	4.59	4.69	4.63	4.56	4.35	4.14	4.75	2.72	3.45	3.80	3.43	3.24	3.48	3.15	3.06	3.00	3.47	3.56
Na_2O	.80	.68	.80	.69	.49	1.10	.68	1.10	1.21	1.30	1.84	1.28	.42	.40	.98	.81	.63	.48
K_2O	1.31	1.27	1.41	1.25	.95	1.31	1.10	1.30	1.52	1.70	1.74	1.45	1.05	.79	1.35	1.21	.95	.96
Total	83.13	83.44	84.43	81.23	80.90	82.37	83.63	76.89	91.37	90.04	92.57	87.98	88.07	75.67	79.30	80.12	83.36	86.30
	Number of atoms on the basis of 72 oxygens																	
Si	28.836	28.795	28.074	28.135	28.309	28.091	28.224	29.783	29.592	29.147	29.317	29.552	29.491	29.366	29.350	29.447	29.375	29.397
Al	7.457	7.620	8.396	8.321	8.229	8.279	8.243	6.705	6.924	7.323	7.102	6.971	7.303	7.423	7.237	7.231	7.337	7.371
Fe	--	--	.153	.160	.214	.288	.151	.000	.000	.000	.000	.000	.000	.000	.000	.000	.000	.000
Ca	2.268	2.305	2.262	2.313	2.205	2.077	2.338	1.442	1.537	1.728	1.518	1.502	1.601	1.688	1.575	1.523	1.690	1.674
Na	.712	.608	.709	.638	.451	1.002	.602	1.051	.979	1.067	1.473	1.070	.349	.383	.911	.747	.557	.411
K	.769	.741	.820	.756	.573	.783	.643	.818	.808	.920	.918	.802	.577	.504	.829	.728	.549	.539
Si/Al	3.82	3.78	3.34	3.38	3.44	3.39	3.42	4.44	4.27	3.98	4.13	4.24	4.04	3.96	4.06	4.07	4.00	3.99

1 Analyst: M. H. Beeson, U.S. Geological Survey.
2 Analyst: J. R. Boden, U.S. Geological Survey.
3 Mn looked for but not found.
4 Mg and Ti looked for but not found.
5 Groundmass analysis; other analyses are open-space fillings.

17.4 m (table 3) belong to group I, heulandite, and subgroup C, intermedite heulandite.

Electron microprobe chemical analyses of clinoptilolite from 21.3 and 22.4 m (table 3) that showed no change in X-ray pattern following heat treatment had higher Si/Al atomic ratios (3.96–4.44), lower SD (Ca) (1.44–1.73), and a wider range of SD/SM (Ca/(Na + K)) (0.63–1.90) than the 17.4 m sample. The Si/Al and SD/SM ratios correspond with the Alietti and others' (1977) refinement of Alietti's (1972) and Boles' (1972) values for clinoptilolite, but the divalent cation values are ambiguous in that they fall between clinoptilolite and intermediate heulandite values given by Boles (1972). According to Hawkins' (1974) classification, both samples are group II, clinoptilolites; however, they range between subgroup C (intermediate heulandite) and subgroup D (clinoptilolite).

Separation of the Y–6 heulandite-group zeolites into two fairly distinct chemical groupings (subgroup C, intermediate heulandite, and subgroup D, clinoptilolite) is seen in a diagram of Si/Al atomic ratios plotted against (Na + K)/(Na + K + Ca) (fig. 8). This plot also contains subgroup E, clinoptilolites, from drill holes C–I (D. E. White, unpub. data, 1967; Fenner, 1936), Y–1 (Honda and Muffler, 1970; M. H. Beeson, unpub. data, 1978), and Y–7 and Y–8 (Keith and others, 1978b) and subgroups B(?) through E, intermediate heulandite and clinoptilolite from Y–2 (Bargar and Beeson, 1981). A ternary plot of Ca, K, Na coefficients (fig. 9) displays the same kind of chemical grouping with cores C–I, Y–1, Y–7, Y–8, and a few Y–2 subgroup E, clinoptilolites all plotting along the sodium-potassium join and subgroups C and D, clinoptilolite and intermediate heulandite, analyses from Y–6 generally having a Ca content that falls in the gap between the subgroups B–E minerals from Y–2.

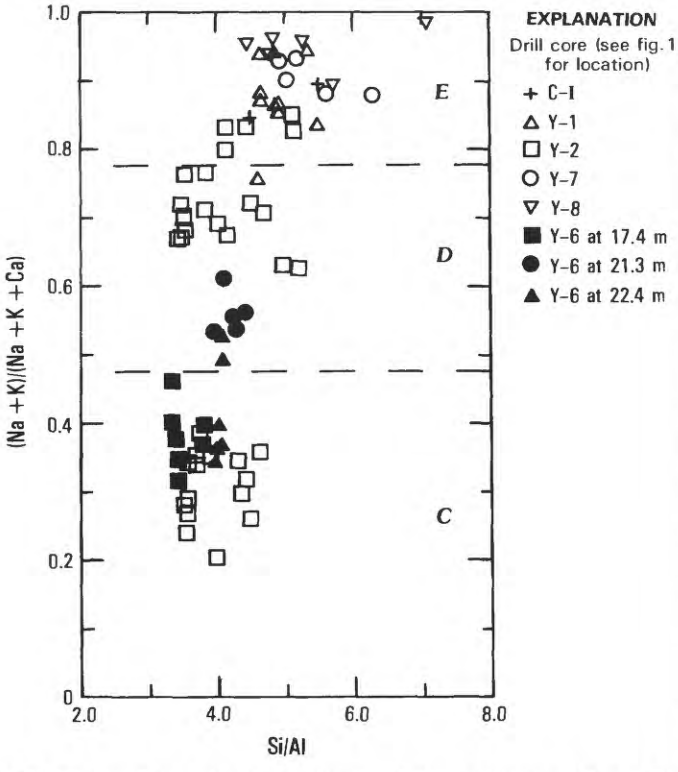

FIGURE 8.—Plot showing atomic Si/Al ratio vs (Na + K)/(Na + K + Ca) for heulandite-group zeolites from Y–6 and other Yellowstone drill cores. Subgroups C, D, and E are based on Hawkins' (1974) classification; dashed boundaries are approximate.

DACHIARDITE

Dachiardite is a zeolite mineral that has been reported from only a few locations in Canada, Italy, Japan, and the United States from hydrothermally altered pegmatite, basalt cavities, and a silico-carbonatite sill (Alberti, 1975; Sheridan and Maisano, 1976; Wise and Tschernich, 1978; Bonardi and others, 1981). The mineral also occurs as open-space fillings or as an alteration product of glass in the glacial sediments and rhyolitic rocks of four Yellowstone drill cores (Y–2, Y–3, Y–6, and Y–13) (Keith and others, 1978a; Bargar and others, 1981; Bargar and Beeson, 1981). In Y–6, dachiardite crystals, identified by X-ray diffraction, fill cavities in association with clinoptilolite, calcite,

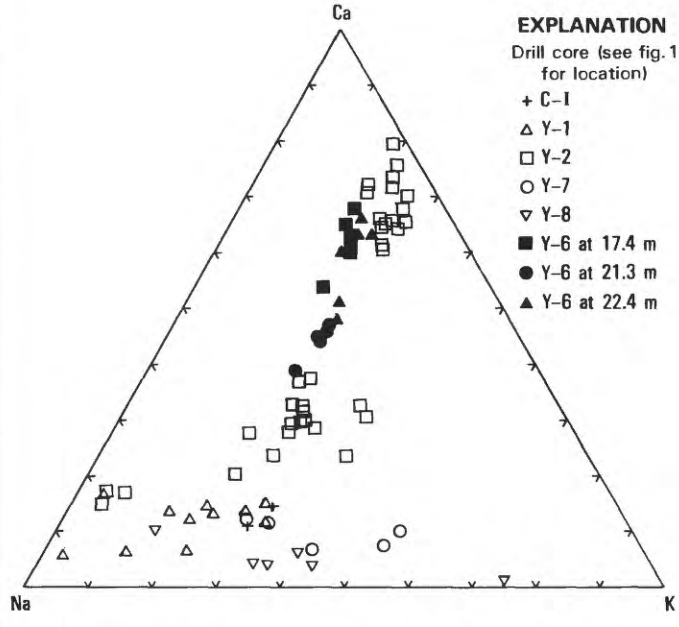

FIGURE 9.—Ca-K-Na ternary diagram for heulandite-group zeolites from Y–6 and other Yellowstone drill cores.

quartz, mordenite, or smectite in three widely separated samples at depths of 21.2, 72.2, and 98.1 m.

The crystal habit of dachiardite has been variously described as eight-sided, blocky cyclic twins; bushlike groups of thin blades that may display polysynthetic twinning; or parallel or divergent fibrous crystals (Wise and Tschernich, 1978; Bonardi and others, 1981). SEM micrographs of core Y–6 dachiardite crystals show short, stubby, parallel growths of polysynthetically twinned(?) bladed crystals (Bargar and others, 1981, fig. 19) or acicular needles that appear to consist of polysynthetic twins of bladed crystals (figs. 10, 11).

Chemical analyses of dachiardite reported by Wise and Tschernich (1978) and Bonardi and others (1981) show considerable variation in exchangeable cation content and a division into Na-rich and Ca-rich varieties. An analysis of dachiardite from drill core Y–2 (Bargar and Beeson, 1981) is calcium rich. Chemical analyses were not obtained for core Y–6 dachiardite; however, a qualitative chemical analysis by SEM of a sample from 98.1 m showed only Si, Al, and Ca.

MORDENITE

Mordenite is the most abundant zeolite mineral in the Y–6 drill core. Mordenite has a sporadic distribution down to 43.8 m and below 89.6 m (fig. 2), but it is very common between those depths as white matted fibrous crystals, clusters of radiating fibers, or individual needles (see figs. 3, 5, 10, 11, 17, 18a, and 19) that line cavities, veins, and fractures. Mordenite may be found in association with most of the hydrothermal minerals shown in figure 2 because it is one of the latest minerals deposited.

CARBONATE MINERALS

CALCITE

White, bladed calcite crystals (up to approximately 2 cm long and < 0.1 mm wide) line cavities and fractures in the drill core from 35.0 m to the bottom of the hole at 152.3 m. Calcite is sparsely distributed in the upper part of the interval but becomes fairly abundant below 122 m (fig. 2). At 35.0 and 35.5 m calcite lines lithophysal cavities and was deposited later than siderite. Elsewhere in the drill core calcite appears to have been deposited in more than one generation. Early(?) deposits of bladed calcite are partly to completely altered to quartz (see fig. 3) or clay minerals (smectite or illite-smectite) with preservation of the bladed morphology. The pseudomorphs may be associated with later pyrite, mordenite, fluorite, or a second generation of white, bladed calcite.

The most intense X-ray diffraction peak

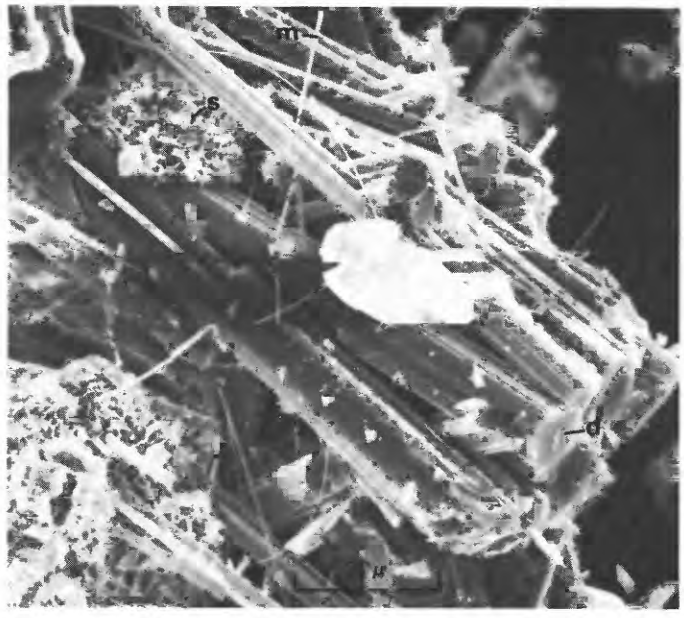

FIGURE 10.—Scanning electron micrograph of polysynthetically twinned acicular aggregates of bladed dachiardite from 98.1 m in drill core Y–6. Fibrous mordenite (m) and boxwork clusters of platy smectite (s) crystals partly coat the striated dachiardite (d) needles.

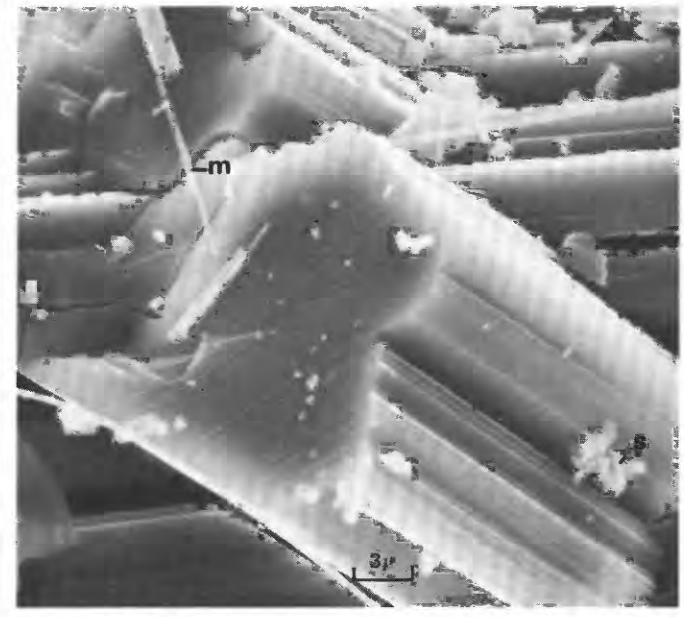

FIGURE 11.—Scanning electron micrograph showing a closeup of acicular aggregates of polysynthetically twinned bladed dachiardite from 98.1 m in drill core Y–6. The monoclinic dachiardite crystals are partly coated by fibrous mordenite crystals (m) and smectite (s).

TABLE 4.—*X-ray diffraction data for Y-6 carbonate minerals, compared with J.C.P.D.S.[1] data for calcite, manganese-calcite, and rhodochrosite*

[Intensites are not listed for Y-6 samples but are about the same as equivalent J.C.P.D.S. minerals]

	Calcite (5-586)[1]		Calcite Y6-125.6[2]	Mn-calcite Y6-44.5[2]	Mn-calcite Y6-40.4[2]	Mn-calcite (2-714)[1]		Ca-rhodochrosite Y6-65.1[2]	Rhodochrosite Y6-65.5[2]	Rhodochrosite (7-268)[1]	
hkl	d(A)	I	d(A)	d(A)	d(A)	d(A)	I	d(A)	d(A)	d(A)	I
012(102)	3.86	12	3.84	3.83	3.77	--	--	3.69	3.65	3.66	35
104	3.035	100	3.02	3.01	2.96[3]	2.95	100	2.88	2.84	2.84	100
006	2.845	3	2.83	2.83	2.76	--	--	2.66	2.61	--	--
110	2.495	14	2.49	2.48	2.45	2.40	30	2.40	2.39	2.39	20
113	2.285	18	2.28	2.28	2.23	2.24	50	2.19	2.17	2.172	25
202	2.095	18	2.09	2.09	2.05	2.04	40	2.02	2.00	2.000	25
024(204)	1.927	5	--	--	--	--	--	1.85	1.83	1.829	12
018(108)	1.913	17	1.91	1.90	1.89	1.85	80	1.80	-	1.770	30
116	1.875	17	1.87	1.86	1.86	1.81	70	1.79	1.76	1.763	35
009	--	--	--	--	1.83	--	--	--	--	--	--
211	1.626	4	1.62	1.62	1.60	--	--	1.57	1.56	1.556	2
122	--	--	--	--	--	--	--	--	--	1.533	14
212	1.604	8	1.60	1.60	1.57	1.56	40	1.55	1.53	--	--
1010	1.587	2	1.58	--	1.54	--	--	1.49	--	--	--
$\overline{214}$	1.525	5	--	--	1.50	1.48	40	1.47	--	1.452	2
--	--	--	1.52	--	--	--	--	--	--	--	--
208	1.518	4	--	--	1.48	--	--	--	--	1.423	1
119	1.510	3	1.51	1.51	--	--	--	--	--	--	--

[1] Joint Committee on Powder Diffraction Standards (J.C.P.D.S.) card numbers.
[2] Sample numbers in meters. Analyses were made at 1°/minute and the data corrected to a quartz internal standard. Accuracy is probably about ± 0.01° 2â.
[3] X-ray data also show an additional carbonate phase with a d(104) X-ray peak at 2.88 A.

d(104)) for pure synthetic calcite occurs at 3.035 A (table 4, column 1). In nine X-ray diffraction patterns of Y-6 calcite, the d(104) peak was measured at 3.02 A (table 4, column 2) to 3.03 A, which indicates that the calcite is not a pure end member and that it undoubtedly contains minor manganese or iron. No microprobe analyses were obtained for this material; however, analyses of a sample from 44.5 m with a d(104) X-ray peak of 3.01 A (table 4, column 3) contains about 8 to 10 mole percent $MnCO_3$ (fig. 12).

MANGANESE-CALCITE

Late deposits of white, hydrothermal manganese-calcite occur in a few fractures and vugs from 40.3 to 63.8 m that are lined by one or more of the following earlier minerals: chalcedony, hematite, apatite, or mordenite. In this report, the term manganese-calcite is defined as a Ca-Mn carbonate containing less than about 50 mole percent $MnCO_3$, similar to the "manganocalcite" studied by Krieger (1930). The most intense X-ray diffraction peak, (d(104)) for this part of the calcite-rhodochrosite solid-solution series, decreases from 3.005 A to 2.948 A with increasing manganese content according to Krieger's data. Core Y-6 manganese-calcite has a d(104) peak that varies from about 3.01 A to 2.96 A (table 4, columns 3 and 4), and the corresponding microprobe analyses (table 5 and fig. 12) show a range of approximately 7 to 35 mole percent $MnCO_3$.

Manganese-calcite (manganocalcite) has been described in two reports (Levison, 1916; Omori and Yamaoka, 1954) as having a "columnar" or "towery" structure. No illustrations were given by Levison for his "columnar manganocalcite"

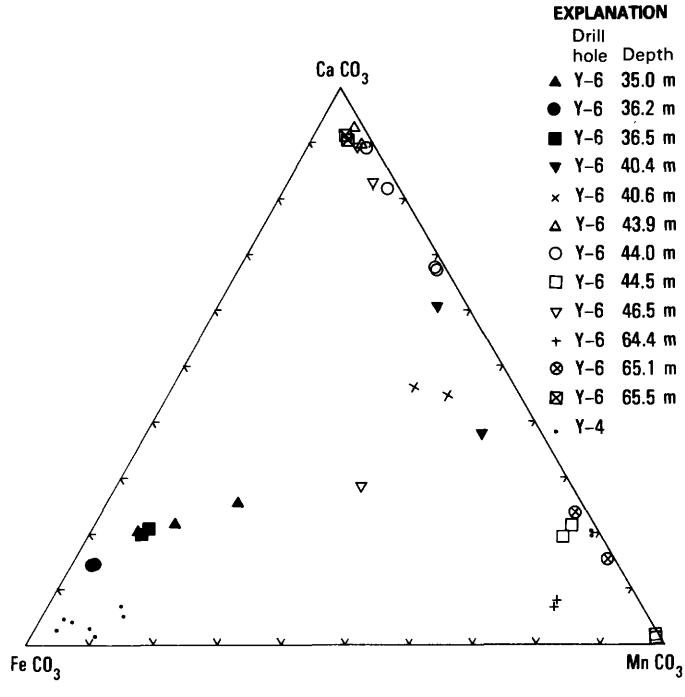

FIGURE 12.—$CaCO_3$-$MnCO_3$-$FeCO_3$ ternary diagram for carbonate minerals from Y-6 drill core. Y-6 data from table 5; Y-4 carbonate microprobe data from T. E. C. Keith and M. H. Beeson, unpub. data, 1979.

TABLE 5.—*Microprobe analyses of carbonate minerals from Y-6 drill core*

[Analyst: M. H. Beeson, U.S. Geological Survey. Looked for but not found: Mg]

Sample No.[1]	Y6-35.0	Y6-35.0	Y6-35.0	Y6-36.2	Y6-36.2	Y6-36.5	Y6-36.5	Y6-40.4	Y6-40.4	Y6-40.6	Y6-40.6	Y6-43.9	Y6-43.9	Y6-44.0	Y6-44.0	Y6-44.0
Mineral[2]	S	S	S	S	S	S	S	M-C	C-M-F	C-M-F	C-M-F	M-C	M-C	M-C	M-C	M-C
								Weight percent								
FeO	33.98	46.02	41.74	51.91	51.06	46.23	45.17	3.12	6.04	10.43	7.59	1.02	1.28	1.19	.93	1.16
MnO	12.68	4.79	7.86	1.92	2.28	4.95	5.74	22.94	34.53	25.08	28.82	3.83	5.60	10.38	6.39	20.33
CaO	12.61	10.06	10.84	7.27	7.29	10.22	10.52	31.72	19.52	24.09	23.42	50.21	48.40	41.52	46.76	35.43
ZnO	.17	.26	.17	.21	.21	.36	.21	.16	.22	.20	.20	--	--	.08	.12	.12
CO_2[3]	40.60	38.87	39.39	38.69	39.16	38.24	38.36	42.06	39.69	40.20	39.97	44.94	44.72	46.83	45.80	42.96
Total	100.04	100.00	100.00	100.00	100.00	100.00	100.00	100.00	100.00	100.00	100.00	100.00	100.00	100.00	100.00	100.00
								Number of atoms on the basis of six oxygens								
Fe	1.042	1.446	1.302	1.642	1.606	1.464	1.427	.092	.185	.316	.231	.028	.036	.033	.026	.034
Mn	.394	.153	.248	.062	.073	.159	.184	.682	1.072	.769	.887	.108	.158	.290	.179	.595
Ca	.495	.405	.433	.295	.294	.415	.426	1.193	.766	.935	.912	1.787	1.731	1.465	1.657	1.312
Zn	.005	.007	.005	.006	.006	.010	.006	.004	.006	.005	.005	--	--	.002	.003	.003
C	2.032	1.994	2.006	1.998	2.011	1.977	1.979	2.015	1.986	1.987	1.983	2.038	2.038	2.105	2.068	2.028

Sample No.--	Y6-44.0	Y6-44.5	Y6-44.5	Y6-46.5	Y6-46.5	Y6-46.5	Y6-64.4	Y6-64.4	Y6-65.1	Y6-65.1	Y6-65.5	Y6-65.5	Y6-65.5	Y6-65.5	Y6-65.5	Y6-65.5
Mineral-----	M-C	M-C	M-C	M-C	C-M-F	M-C	F-R	F-R	C-R	C-R	C-R	C-R	R	R	R	R
								Weight percent								
FeO	1.05	2.51	2.50	2.34	20.73	1.57	7.91	8.69	.61	1.18	2.18	3.59	.24	.18	.18	.21
MnO	19.98	3.68	3.37	8.96	24.11	5.49	49.60	49.55	53.61	46.15	46.44	46.71	60.88	62.04	61.78	62.21
CaO	34.21	47.99	48.50	43.73	14.17	47.71	3.94	3.36	7.84	11.78	10.45	9.64	.66	.71	.97	.69
ZnO	.15	.12	.08	.13	.13	.13	.27	.23	.14	.17	.20	.18	.24	.24	.25	.25
CO_2[3]	44.61	45.70	45.55	44.84	40.86	45.10	38.28	38.17	37.80	40.72	40.73	39.88	37.98	36.83	36.82	36.64
Total	100.00	100.00	100.00	100.00	100.00	100.00	100.00	100.00	100.00	100.00	100.00	100.00	100.00	100.00	100.00	100.00
								Number of atoms on the basis of six oxygens								
Fe	.030	.069	.069	.066	.632	.044	.252	.277	.019	.036	.067	.111	.008	.006	.006	.007
Mn	.576	.103	.094	.255	.744	.155	1.600	1.602	1.728	1.430	1.442	1.466	1.979	2.045	2.036	2.055
Ca	1.247	1.700	1.719	1.571	.553	1.701	.161	.137	.320	.412	.410	.383	.027	.030	.040	.029
Zn	.004	.003	.002	.003	.004	.003	.008	.007	.004	.005	.005	.005	.007	.007	.007	.007
C	2.072	2.063	2.058	2.053	2.033	2.049	1.990	1.989	1.964	2.034	2.038	2.018	1.990	1.957	1.956	1.951

[1] Sample numbers correspond to depth in meters.
[2] S=Siderite, M-C=manganese-calcite, C-R=Calcium-rhodochrosite, R=rhodochrosite, F-R=iron-rhodochrosite, and C-M-F=calcium-manganese-iron-carbonate.
[3] CO_2 by difference.

($MnCO_3$ = 16.83 mole percent), but his description suggests a structure similar to the one shown in the scanning electron micrograph of figure 13*A* for Mn-calcite from 40.4 m in core Y–6. A closer view of this sample (fig. 13*B*) shows that the columns consist of closely packed rhombic crystals. The stacked rhombohedrons appear similar to a drawing of "towery manganocalcite" ($MnCO_3$ from 5.16 to 31.4 mole percent) by Omori and Yamaoka (1954). Similarly stacked manganese carbonate crystals are shown in figure 14*A*. The terms "columnar" or "towery" might also apply to this mineral habit. SEM micrographs of the mineral (figs. 14*B* and 14*C*) show that the columns or towers consist of stacks of rounded aggregates of rhombic crystals. Figures 15*A*, 15*B*, and 15*C* show a somewhat different structure for manganese-calcite consisting of a spindle-shaped or fusiform arrangement of columns of stacked crystals.

Manganese-calcite has not been found in other Yellowstone drill cores, although both manganese oxide and travertine are identified in the upper part of Y–2 drill core (Bargar and Beeson, 1981) and manganese oxide and travertine occur in surficial deposits of the Firehole Lake area (in the vicinity of Y–2; see fig. 1) (Allen and Day, 1935) and at Hillside Springs in Upper Geyser Basin (White, 1955). Minor Mn-calcite was identified at 19.2 m (at about 90°C) in drill hole GS-1 and from 51.8 m in drill hole GS-7 (approximately 120°C) at Steamboat Springs, Nev., by Sigvaldason and White (1961, 1962).

Chemical composition of several of the Y–6 carbonate minerals ranges through much of the calcite-rhodochrosite solid-solution series (table 5 and fig. 12) and displays some inhomogeneity within a single sample, but the analyses are consistent with experimental data which indicate that the $CaCO_3$-$MnCO_3$ series is incomplete in the range of about 50 to 80 mole percent $MnCO_3$ at temperatures below 550°C (Goldsmith and Graf, 1957). Kutnahorite, a $CaMn(CO_3)_2$ mineral with a dolomitic structure, has a Ca:Mn atomic ratio of about 1:1 (Frondel and Bauer, 1955). Microprobe analyses of samples from 40.4, 40.6, and 46.5 m plot close to Goldsmith and Graf's miscibility gap (fig. 12), but X-ray diffraction analyses indicate that the three samples do not have a dolomitic structure. All three of the samples have additional microprobe analyses that plot in the Mn-calcite field (one Mn-calcite analysis from 40.6 m is not reported in table 5 or plotted in fig. 12 because of a cation-balance deficiency) and X-ray traces that are characteristic of Mn-calcite (see table 4, column 4); however, all three diffractometer traces contain an extra peak at about 2.85 to 2.89 A, which is interpreted as an inhomogeneity in the crystal structure due to the presence of significant iron.

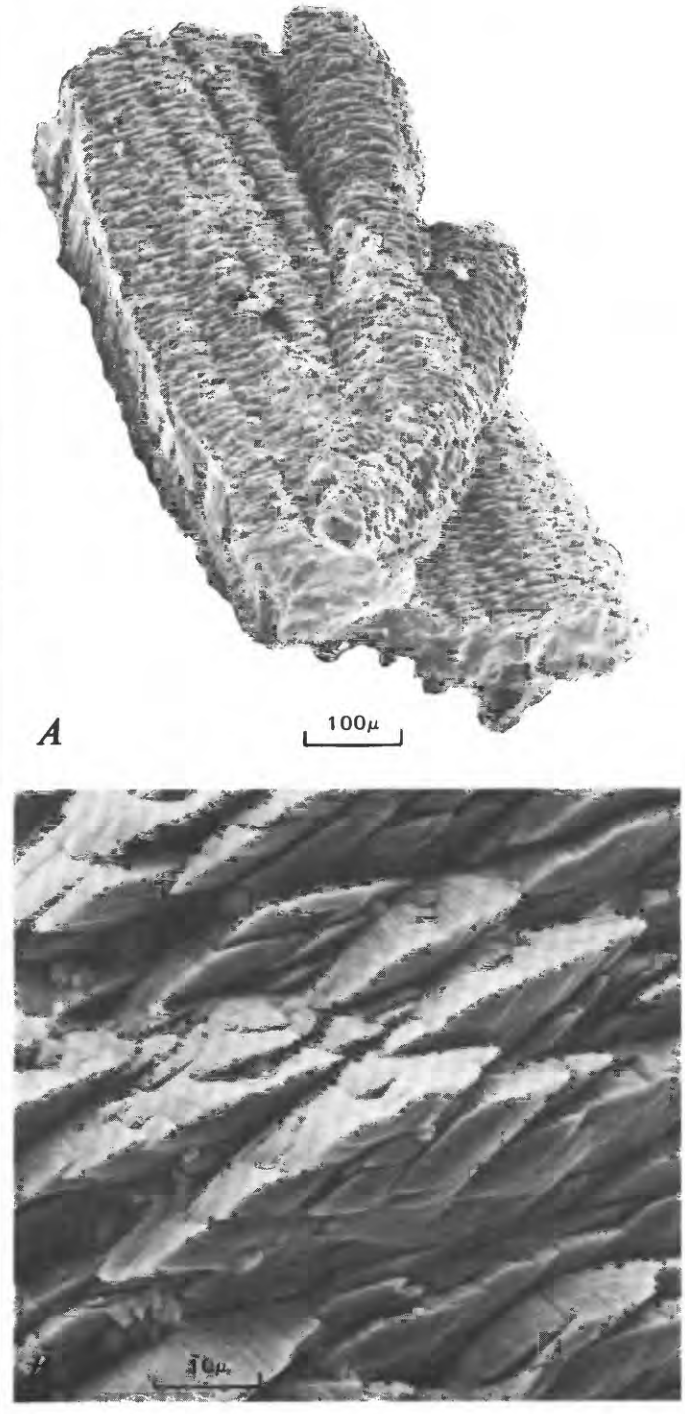

FIGURE 13.—Scanning electron micrographs of *A*, "Columnar" manganese-calcite from 40.4 m in drill core Y–6, and *B*, Closely packed rhombic manganese-calcite crystals that make up the "columnar" structure shown in Figure 13*A*.

X-ray diffraction data for the Y–6 Ca-Mn carbonates show a shift to smaller d values of nearly all X-ray diffraction peaks with increasing manganese content (compare tables 4 and 5, samples Y6–40.4 and 44.5), which records the decrease in the size of the unit cell as smaller manganese atoms substitute for larger calcium atoms in the structure. This relationship was documented for Ca-Mn carbonates by Krieger (1930), who also noted similar differences in the index of refraction and specific gravity with changes in chemical composition.

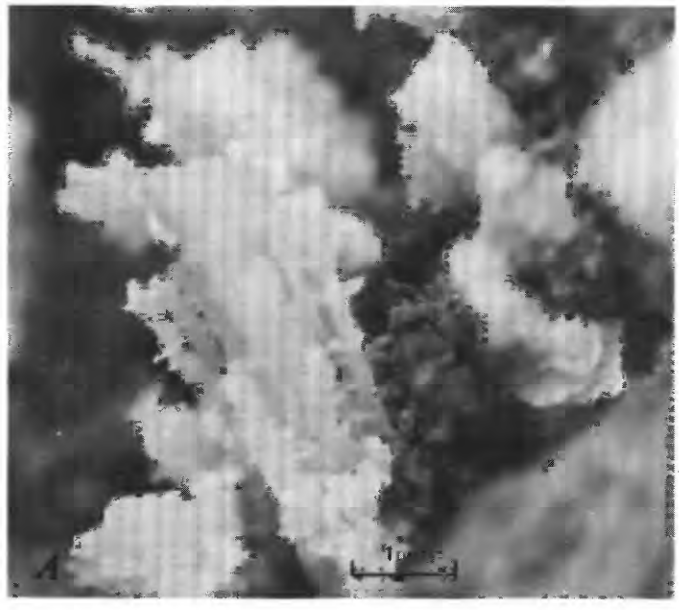

RHODOCHROSITE

Several fractures and cavities between 64.4 and 66.8 m in drill core Y–6 are lined by chalcedony, quartz, disc-shaped aggregates of rhombic manganese-rich carbonate crystals that are white, pale pink, orange, brown, or black, and sometimes later mordenite and chlorite. X-ray diffraction traces of samples from 41.8 and 144.3 m also show the presence of $MnCO_3$ (rhodochrosite), although none was seen with a binocular microscope. The manganese-rich carbonate minerals were subdivided into calcium-rhodochrosite, iron-rhodochrosite, and rhodochrosite on the basis of X-ray diffraction data and microprobe chemical analyses.

Calcium-rhodochrosite from drill core Y–6 has a d(104) X-ray peak at about 2.86 to 2.88 A (Shibuya and Harada, 1976; see table 4, column 6) and contains about 74 to 84 mole percent $MnCO_3$ (fig. 12). Most of the Y–6 microprobe analyses and unpublished Y–4 analyses (M. H. Beeson and T. E. C. Keith, unpub. data, 1982) plot near the upper end of Goldsmith and Graf's miscibility gap and may be metastable, although their data did not contain results from low-temperature studies because of the length of time for such reactions to take place. Temperatures, measured as drilling progressed, for the depth at which rhodochrosite was formed in drill holes Y–6 and Y–4 are 140° and 194°C (White and others, 1975), respectively. Unanalyzed rhodochrosite has also been identified in

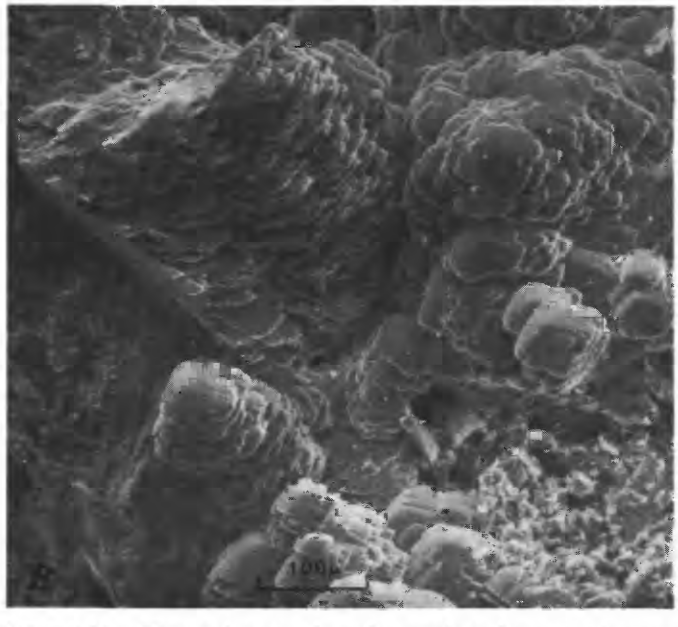

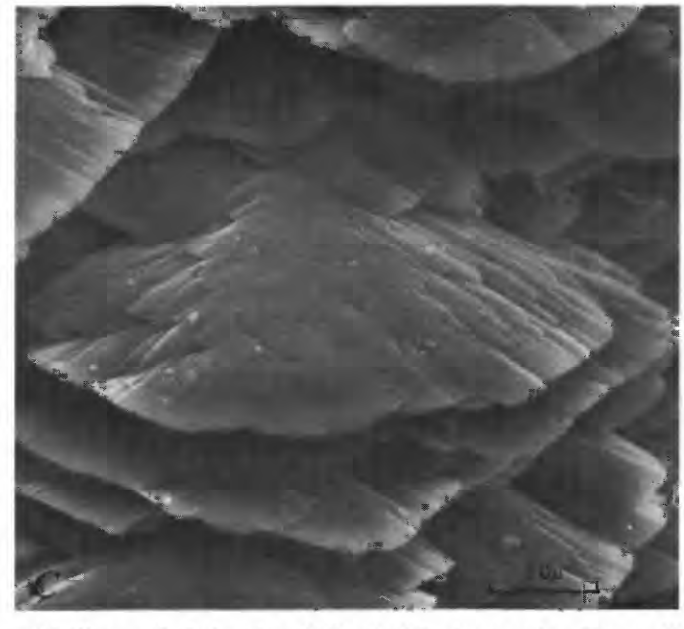

FIGURE 14.—Photomicrograph and scanning electron micrographs of drill core Y–6 showing *A*, Stacked "columnar" or "towery" manganese-calcite crystals lining a cavity at 40.3 m. *B*, Stacked manganese-calcite crystals lining a cavity at 40.6 m. *C*, Stacked rounded aggregate of rhombic manganese-calcite crystals from 40.6 m.

drill core Y–11 (Muffler and Bargar, 1974; Bargar and Muffler, 1982), where the temperature measured during drilling was about 150°C.

Rhodochrosite from the Y–6 drill core has a d(104) X-ray peak at about 2.84 A, which is the same as the Joint Committee on Powder Diffraction Standards (J.C.P.D.S.) (Berry and others, 1974) card for pure synthetic rhodochrosite (compare columns 7 and 8 in table 4), and contains about 98 mole percent $MnCO_3$ (table 5, and fig. 12).

One sample from 64.4 m also has a d(104) peak at 2.84 A; however, repeated microprobe analyses showed the presence of about 12–14 mole percent $FeCO_3$. According to Rosenberg (1963), a continuous solid-solution series exists in the $MnCO_3$-$FeCO_3$ system.

SIDERITE

Pale-yellow to dark-reddish-orange, tiny, curved-surface rhombohedral siderite crystals were identified from 31.6 to 39.0 m and at 46.3 and 49.6 m in Y–6 drill core. Discrete hydrothermal siderite crystals or crystal clusters (fig. 16) occur as cavity or fracture fillings along with earlier hydrothermal marcasite and green smectite and later bladed calcite, mordenite, and kaolinite.

Temperatures at which Y–6 siderite was found ranged from about 80° to 120°C (see fig. 2). This temperature is a little lower than the 130° to 140°C for Y–2 siderite (Bargar and Beeson, 1981), but it is within the range (37° to 130°C) reported by Browne and Ellis (1970) for siderite from Broadlands, New Zealand.

Steiner (1977) indicated that hydrothermal siderite from the Wairakei geothermal area of New Zealand was formed by replacement of hypersthene and hornblende. Y–6 siderite was deposited from a geothermal solution that was apparently rich in ferrous iron as indicated by the

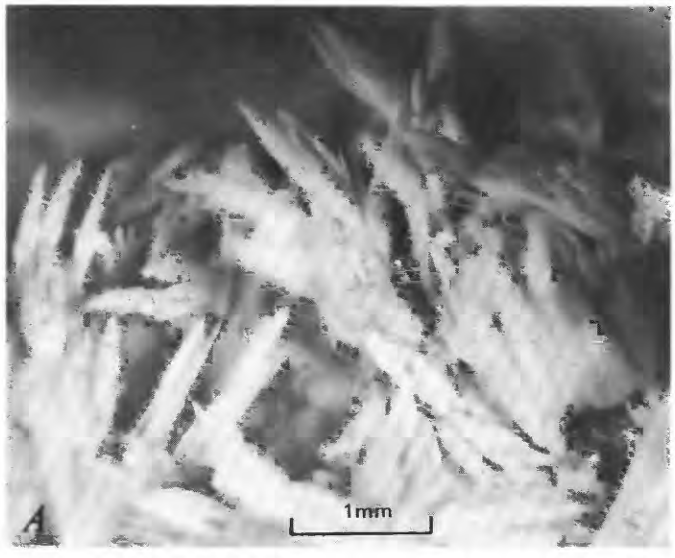

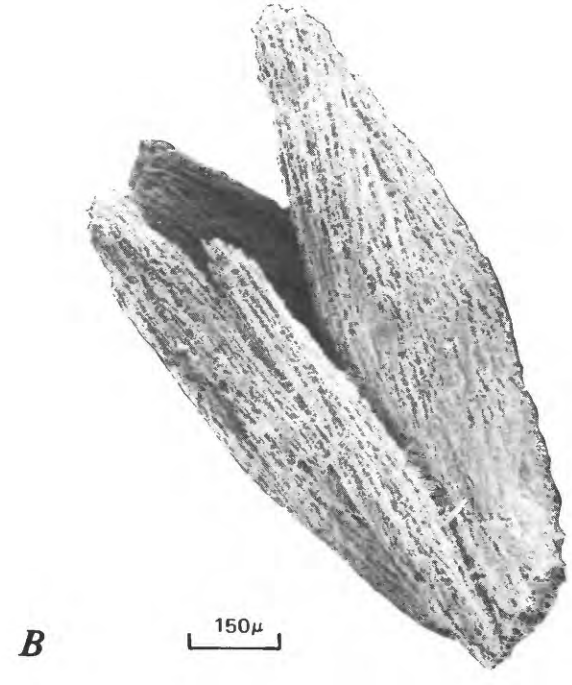

FIGURE 15.—Photomicrograph and scanning electron micrographs of drill core Y– 6 at 44.0 m. *A*, Spindle-shaped manganese-calcite cavity filling. *B*, Spindle-shaped columnar or stacked aggregates of manganese-calcite crystals. *C*, Columnar stacked aggregates of manganese-calcite crystals.

earlier formation of marcasite and green (iron-rich) smectite.

The d(104) X-ray diffraction peak of Y–6 siderite varies from about 2.82 to 2.83 A compared to 2.79 A for synthetic siderite (Berry and others, 1974; J.C.P.D.S. card no. 12-531). X-ray data (d(104) peak) for Y–4 siderite also deviates slightly from pure siderite (T. E. C. Keith, oral commun., 1982). In figure 12, the chemical composition of Y–4 siderite plots closer to the $FeCO_3$ apex than does the Y–6 siderite (siderite samples from both drill cores were chemically analyzed on the same day using the same microprobe). Siderite from both drill cores contains a range of manganese values; the Y–6 siderite also contains significant calcium. In fact, experimental work in the $CaCO_3$-$FeCO_3$ system (Rosenberg, 1963, 1967) indicates that a solid-solution phase of the composition found in Y–6 does not occur at the higher temperatures (300° to 500°C) necessary for reactions to proceed in the laboratory. However, work by Huebner (1969) suggests that the addition of manganese can expand the siderite stability field.

APATITE

Clear to white, euhedral, hexagonal apatite crystals (fig. 17) were found in Y–6 drill core at 40.2 to 40.6 m, where the present temperature interpolated from figure 2 would be about 100°C. The clustered apatite crystals (approximately 0.1 to 1.0 mm diameter) were deposited on fractures and in cavities that contain earlier granophyric quartz and vapor-phase K-feldspar crystals. Paragenesis of the open-space hydrothermal minerals in the recovered core is chalcedony, quartz, marcasite, apatite, quartz, manganese-calcite, mordenite, and smectite.

Hydrothermal apatite has not been identified in other Yellowstone drill cores, but it does occur as pseudomorphs after hornblende and hypersthene, along with chlorite, micaceous clay, quartz, and epidote, in material recovered from drill holes in the Wairakei geothermal area, New Zealand (Steiner, 1977). Minor hydrothermal apatite has also been reported from drill holes in other geothermal areas: Steamboat Springs, Nev. (Sigvaldson and White, 1961); Milos, Greece (Fytykas and others, 1976); Cesano, Italy (Funiciello and others, 1979); and Larderello, Italy (Cavarretta and others, 1980).

Steiner indicated that the New Zealand apatite probably formed from constituents which were

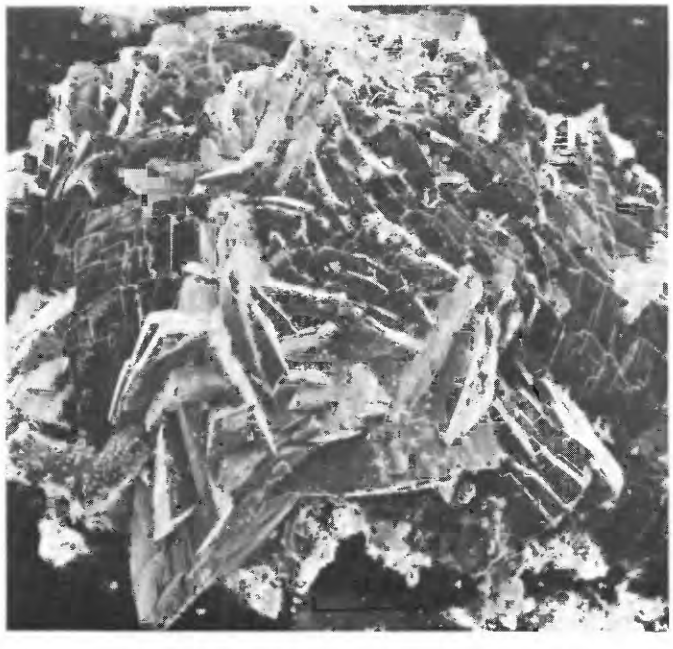

FIGURE 16.—Scanning electron micrograph showing an aggregate of curved rhombic siderite crystals from core Y–6 at 35.0 m.

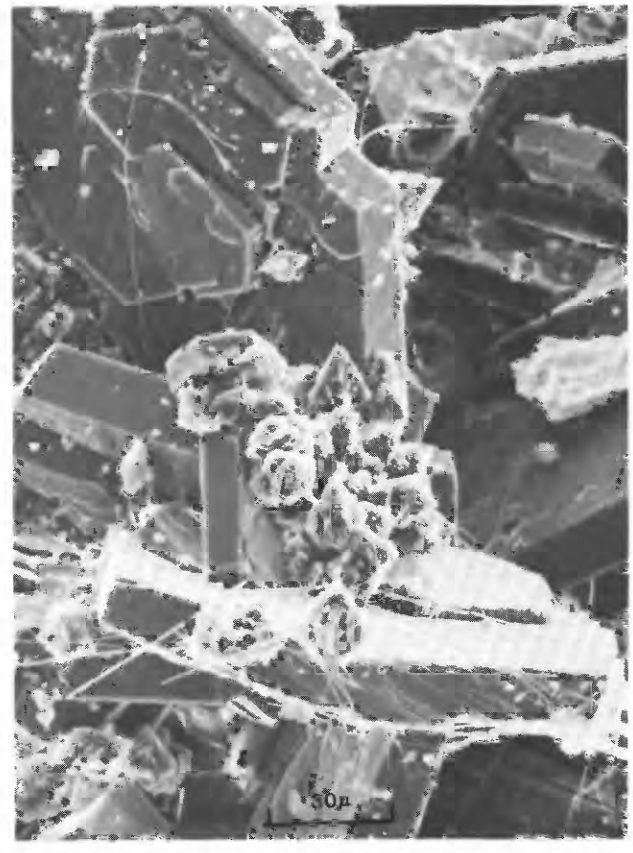

FIGURE 17.—Scanning electron micrograph showing euhedral hexagonal apatite crystals in a core Y–6 cavity at 40.6 m. The apatite crystals are partly coated by later smectite, dipyramidal quartz crystals, and mordenite fibers.

already present in the host rocks and were not introduced by the geothermal fluid. Conversely, the morphology of the Y–6 apatite dictates that it was certainly deposited by circulating hot water. Water from Y–6 was not analyzed for phosphorus (table 1); however, PO_4-P (phosphorus as phosphoric acid) concentrations of 0.7 micrograms per liter were determined from nearby hot springs (Stauffer and Thompson, 1978). These analyses are at the low end of the PO_4-P spectrum (0.7-73 micrograms per liter) for Yellowstone hot-spring waters which, except for travertine-depositing springs, are mostly near saturation with respect to apatite (Stauffer, 1982).

FLUORITE

Fluorite, a common hydrothermal mineral, apparently is uncommon in geothermal areas and has been reported only from Kawah Kamojang, Java, and Yellowstone National Park (Browne, 1978). Open-space fluorite deposits previously have been found in Yellowstone drill cores Y–2 (Bargar and Beeson, 1981), Y–3 (Bargar and others, 1973), Y–4 (D. E. White, written commun., 1982), Y–5 (Keith and Muffler, 1978), Y–11 (Muffler and Bargar, 1974; Bargar and Muffler, 1982), and Y–13 (Keith and others, 1978a). Sporadic fluorite also occurs below 71.7 m in drill core Y–6, where temperatures measured during drilling were about 140° to 180°C. Clear to white, euhedral, octahedral (fig. 18*A*) (rarely cubic (fig. 18*B*) twinned penetration cubes or hexoctahedrons) fluorite crystals range in size from about 0.1 to 4.0 mm. Several fractures and irregular open-space fillings contain deposits as thick as 1.0 cm of crystalline to massive fluorite in association with earlier chalcedony, marcasite, calcite, and quartz and later pyrite, smectite, and mordenite.

Richardson and Holland (1979) indicated that hydrothermal fluorite can form by several mechanisms, the most important of which is decreasing solubility related to decreasing temperature. Precipitation of fluorite in drill core Y–6 probably resulted from dilution and a decrease in temperature due to mixing of cold meteoric water with the geothermal water.

CLAY AND MICA MINERALS

SMECTITE

Smectite is the predominant clay mineral from about 17.4 to 126.9 m in the Y–6 drill core (see fig. 2). Varicolored smectite was deposited in vugs and fractures and forms as an alteration product of glass, in the upper part of the Scaup Lake flow,

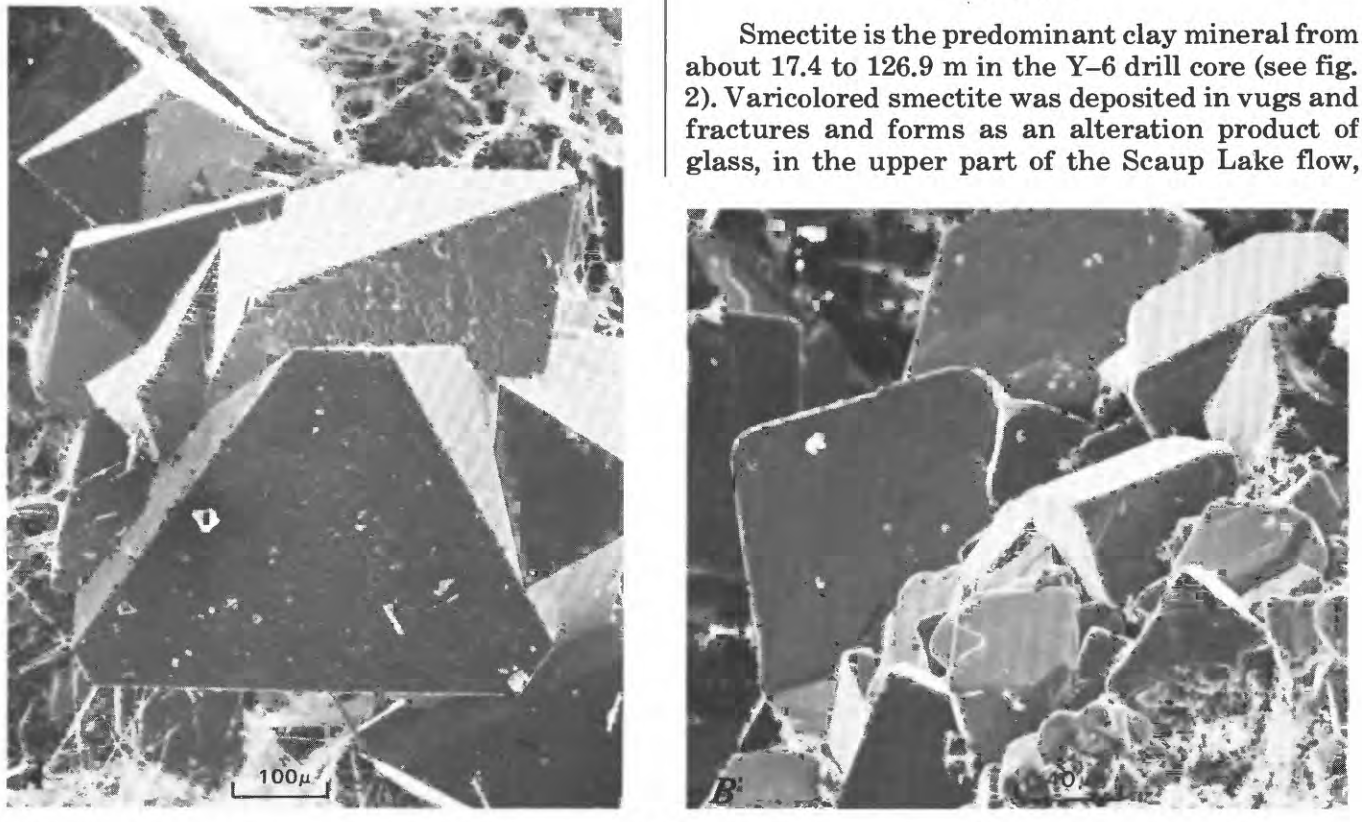

FIGURE 18.—Scanning electron micrographs of drill core Y–6 showing *A*, Cluster of octahedral fluorite crystals deposited in a cavity at 78.5 m. Fibrous mordenite is a later deposit. *B*, Cubic fluorite crystals from 91.7 m. Smectite partly coats the fluorite.

and in most mafic crystals and occasional plagioclase phenocrysts. Open-space smectite fillings are generally deposited later than early quartz deposits (see fig. 4), and examples were found indicating that smectite can coat any of the later forming hydrothermal minerals but does not consistently do so. The clay deposits are occasionally pseudomorphous after earlier deposited bladed calcite or fibrous mordenite. More commonly, clusters of sheetlike smectite crystals occur as partial coatings on earlier hydrothermal minerals (figs. 19 and 20).

X-ray diffraction analyses of more than 100 samples show that the smectite basal (001) spacing varies from about 12 to 15 A and expands to about 17 A when placed in an atmosphere of ethylene glycol at 60°C for 1 hour. According to Grim (1968), the lower part of the range (approximately 12.5 A) corresponds to Na^+ as the exchangeable cation, and, in the upper end (approximately 14.5-15.5 A), Ca^{2+} should be the exchangeable cation. The two exchangeable cations show no discernible distribution pattern in the upper part of the drill core, although sodium appears to be slightly dominant. Below about 48.8 m, calcium is almost exclusively the dominant cation.

A single chemical analysis of a clay veinlet at 29.7 m, by electron microprobe (J. R. Boden, unpub. data, 1981), shows that the clay mineral contains 53.23 percent SiO_2, 18.98 percent Al_2O_3, 5.88 percent FeO, 1.16 percent CaO, 0.60 percent Na_2O, 2.50 percent K_2O, and no MgO or TiO_2 (total = 82.35 weight percent). The analysis contains more potassium than either calcium or sodium and may be of a mixed-layer illite-smectite, although only smectite was identified in three separate X-ray diffraction analyses from this interval.

ILLITE-SMECTITE

Mixed-layer illite-smectite occurs in two zones, one near the top and the other near the bottom of the Scaup Lake flow. In the upper zone green mixed-layer clay was deposited on a few fractures between 23.2 and 30.9 m and has an air-dried basal (001) X-ray diffraction peak at about 11.4 A which splits into two peaks at about 17.5 A and 9.8 A after glycolation at 60°C for 1 hour. The low, broad, asymmetrical X-ray peaks are poorly defined and difficult to confidently measure but appear to correspond to randomly interstratified illite (glycol)-smectite of approximately 40 to 60 percent illite (see fig. 4.7 in Reynolds, 1980, and fig. 3.1 in Hower, 1981).

The lower mixed-layer clay zone (below 126.9 m) consists of white to buff or green cavity or fracture fillings and clay replacing plagioclase and mafic phenocrysts. This interval appears to contain a randomly interstratified illite (glycol)-smectite with an air-dried X-ray basal (001) peak of 12.5 A which splits into a 16.8–A peak and a

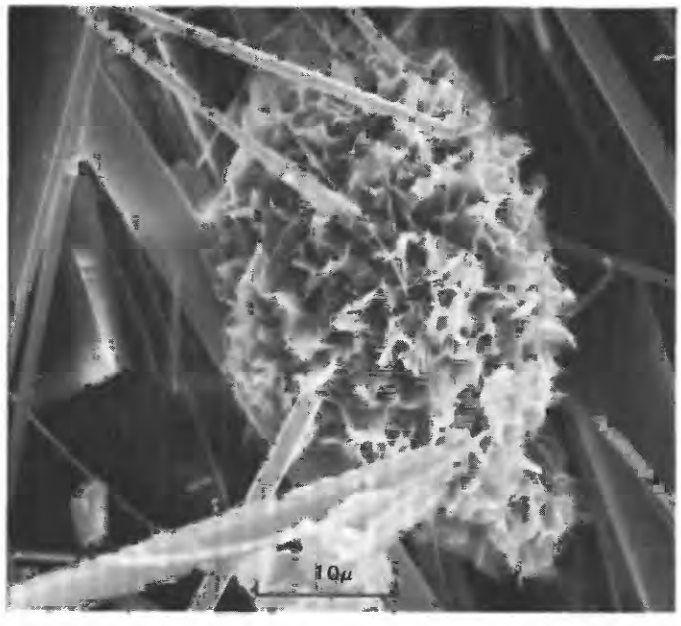

FIGURE 19.—Scanning electron micrograph showing a boxwork cluster of sheetlike smectite crystals coating mordenite fibers in core Y–6 at 98.1 m.

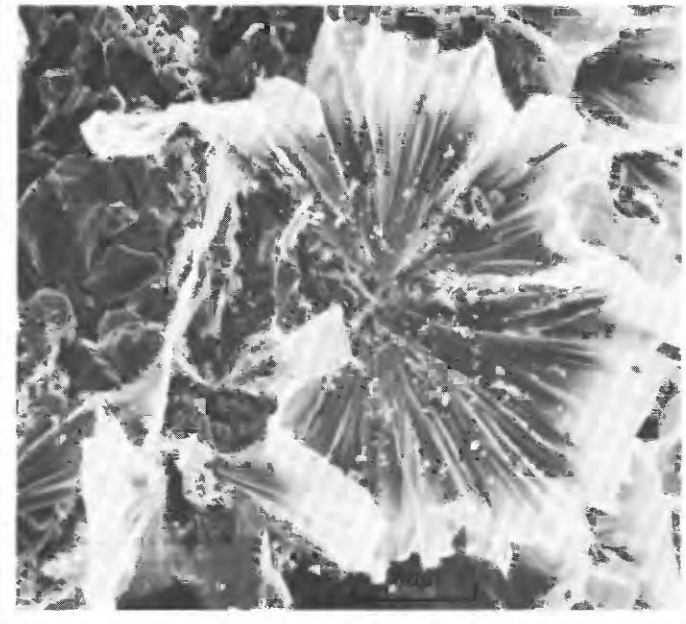

FIGURE 20.—Scanning electron micrograph showing radiating cluster of sheetlike smectite crystals coating quartz crystals in core Y–6 at 91.8 m.

9.2–A peak following glycolation and, according to figure 3.1 of Hower (1981), would contain approximately 40 percent illite. The lower zone also has an ordered interstratified illite (glycol)-smectite with an air-dried basal (001) X-ray peak at about 11.2 A that splits into two peaks at 12.9 and 9.7 A after glycolation and appears to contain about 60–80 percent illite according to figure 3.2 of Hower (1981).

KAOLINITE

Kaolinite fills cavities and lines fractures in the Y–6 drill core between 23.4 and 42.7 m, where the temperature measured during drilling was about 60°to 110°C, and at 81.2 and 87.7 m in association with earlier deposited green smectite. Snowy white kaolinite balls that mostly coat the roofs of lithophysal cavities consist of a mat of vermicular growths of stacked platy crystals (fig. 21). According to Lahodny-Sare and others (1981), some variation of this crystal habit is typical for natural and synthetic kaolinites. The presence of kaolinite concentrated mainly in the upper 40 m (at the top of the Scaup Lake flow) suggests that the mineral may have been produced by surficial acid alteration (Browne and Ellis, 1970) presumably before Pinedale sediments were deposited, although this is not likely for sparse kaolinite found between 80 and 90 m.

CHLORITE

A small amount of scattered chlorite occurs in the drill core from 37.6 to 55.3 m; below 55.3 m chlorite was found in nearly every sample studied. In core Y–6 chlorite is a common alteration product of mafic phenocrysts and is associated with hematite, magnetite, pyrite, and 10–A mica. Chlorite also lines fractures and cavities at scattered locations in the drill core. Open-space chlorite appears to have formed at various times and may be an early mineral associated with red chalcedony and pyrite, a very late mineral coating mordenite, or a deposit along with other clay minerals somewhere in between. Numerous X-ray diffraction analyses of chlorite show that the (002) and (004) reflections are usually strong and that the (001) and (003) peaks are weak. These peak intensities suggest that the mineral is an iron-rich chlorite (Grim, 1968), as might be expected from its frequent association with pyrite and red iron oxide-stained chalcedony.

10-A MICA

Figure 2 shows scattered minor amounts of a 10–A mica between 37.6 m and the bottom of the drill hole at 152.3 m. The mineral identification is based on a low-intensity, sharp, 10–A X-ray diffraction peak, and the mica is listed in figure 2 as a hydrothermal mineral because it was found at 145.5 m in some abundance intergrown with chlorite in a vesicle filling.

IRON OXIDES AND SULFIDES

HEMATITE AND GOETHITE

Orange, red, or reddish-brown iron oxide is fairly abundant throughout most of the Y–6 drill core (see fig. 2) and occurs as coatings of fractures and cavities and alteration of mafic phenocrysts. X-ray diffraction analysis of selected samples indicates that hematite is the prevalent iron oxide phase. Goethite was only found in a single sample at 46.9 m as a thin yellow-brown earthy or clayey fracture coating (X-ray trace also shows presence of smectite). In drill core Y–6, hematite, an early hydrothermal mineral, is commonly seen coating vapor-phase K-feldspar and granophyric quartz and colors some early open-space chalcedony deposits. All other open-space hydrothermal minerals appear to be deposited later than hematite.

FIGURE 21.—Scanning electron micrograph showing platy crystals of vermicular stacked kaolinite from cavity filling in core Y–6 at 36.5 m.

MARCASITE

Brass-yellow (though frequently darkened due to post-drilling(?) oxidation) hexagonal platelets (fig. 22) or larger (up to approximately 0.5 cm) "cockscomb" aggregates of marcasite crystals were found in drill core Y–6 at depths of 31.6 to 40.3 m, 49.6 m, 58.0 to 71.7 m, and 132.6 to 134.8 m. In the upper zone, marcasite occurs mainly in lithophysal cavities along with one or more of the later deposited minerals: siderite, calcite, smectite, or kaolinite. A fracture system at the base of the interval contains hematite-coated vapor-phase K-feldspar crystals, red chalcedony, brass-yellow "cockscomb" marcasite, pyrite, apatite, manganese-calcite, mordenite, and smectite. Cavities in the middle zone contain a few hexagonal marcasite crystals in addition to one or more of the above minerals and fluorite (at 71.7 m). Near-vertical fractures in the lower zone are coated by illite-smectite and yellow fine-grained sulfides (marcasite and pyrite in X-ray). Hexagonal marcasite blades are also disseminated throughout the groundmass of the remainder of the bottom zone.

X-ray diffraction traces of samples from each of the three zones show that all of the marcasite analyzed below approximately 40 m contains a pyrite component. Marcasite is regarded as metastable with respect to pyrite at low temperature (Taylor, 1980) and converts to pyrite at temperatures above 160°C. According to McKibben (1979), this is a useful temperature indicator in the Salton Sea geothermal system. Marcasite was reported from Tongonan, Philippines, and the New Zealand volcanic zone (Browne, 1978), and from Steamboat Springs, Nev. (Sigvaldson and White, 1962). In the last geothermal area, drill holes GS–5 and GS–7 both contain marcasite at temperatures lower than approximately 140°C. The temperature range at which marcasite was found in Y–6 drill core was 80° to 170°C.

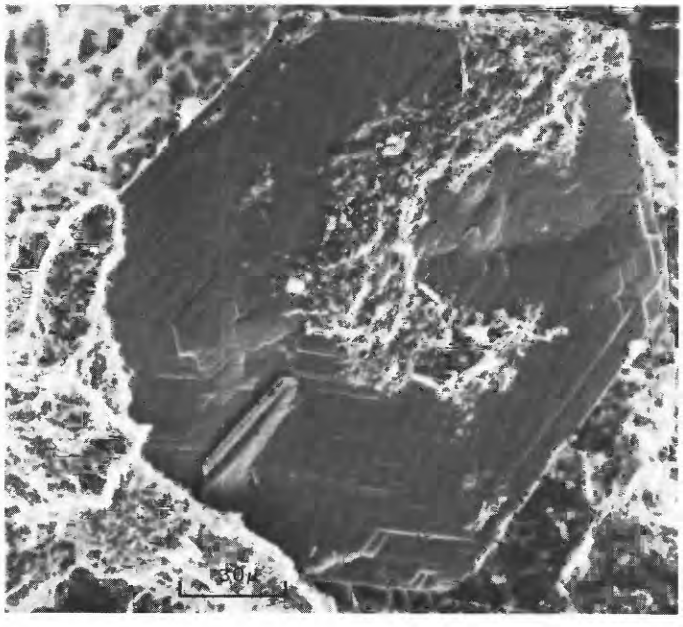

FIGURE 22.—Scanning electron micrograph showing hexagonal platelet of marcasite that is partially coated by smectite in core Y–6 at 36.5 m.

PYRITE

Nearly every piece of Y–6 drill core studied contains at least a trace of pyrite (see fig. 2). Pyrite is found most commonly as an open-space filling that appears to have been deposited during two separate episodes. Earliest formed pyrite occurs as tiny cubic crystals or irregular masses that line the outer margins of vugs and fractures and were deposited in association with hematite and red chalcedony. Euhedral pyrite cubes are also found in cavities on top of clear quartz crystals that formed later than hematite and red chalcedony. Very tiny pyrite crystals are disseminated in the groundmass of a few sections of core. Pyrite also appears to have formed as one of the alteration products of mafic minerals along with hematite, chlorite, and clay.

SUMMARY AND DISCUSSION

The Y–6 drill hole penetrated a mantle of Pinedale glacial sediments above rhyolite of the Scaup Lake flow (K-Ar date approximately 265,000 years B.P.; J. D. Obradovich and R. L. Christiansen, unpub. data, 1973) of the Upper Basin Member of the Plateau Rhyolite. Some of the glassy rhyolite groundmass was hydrothermally altered to zeolite and clay minerals, but most was devitrified to α-cristobalite and sanidine and is characterized by microspherulitic texture. Lithophysal cavities and other vugs are lined by granophyric quartz and vapor-phase minerals. Abundant hydrothermally mineralized fractures in the drill core are devoid of vapor-phase minerals and were probably not formed during emplacement and cooling of the lava flow.

Conductive heat-flow calculations by Fournier and others (1976) suggest that current hydrothermal activity in Yellowstone Park began about 150,000 years ago, which coincides with timing of the Mallard Lake doming, associated fracturing, and extrusion of voluminous lava flows

(Eaton and others, 1975). Late Bull Lake kame deposits that formed approximately 140,000 years ago in the vicinity of the Y–6 drill hole are hydrothermally cemented and are overlain by uncemented deposits of Pinedale age (≥45,000 to 14,000 years B.P.) (Waldrop, 1975; Pierce and others, 1976).

Calculated porosity of seven representative rock samples from the Y–6 drill core is generally low (about 3 to 15 volume percent) except for one sample of pumiceous rhyolite flow breccia which has a porosity of 29 volume percent. Chemical analyses of the upper pumiceous, vitrophyric, and lithophysal part of the Scaup Lake flow show considerable variation in major-oxides content; below approximately 45 m the whole-rock chemistry does not appear to vary significantly from an analysis of unaltered Scaup Lake rhyolite given in Keith and others (1978b). Permeability in the lower two-thirds of the drill core was high due to the abundance of fractures, although many of the fractures are nearly or completely closed (self-sealed) by deposition of hydrothermal minerals (dominated by chalcedony).

Several pieces of drill core contain fracture zones, in which the outlines of chalcedony-enveloped rock fragments can be matched readily with adjacent wallrock. Fracturing and subsequent fracture filling by hydrothermal minerals in Y–6 appear much the same as that described for drill core Y–5 by Keith and Muffler (1978). Their interpretation suggests that the Y–5 fractures are related to the Mallard Lake resurgent doming and were filled immediately after formation by deposits of amorphous or poorly ordered silica. These silica fracture fillings were recrystallized later to chalcedony. A similar process involving Mallard Lake doming and subsequent surge of silica-saturated water may be responsible for chalcedony fracture fillings in the Y–6 drill core.

The chemical composition of Y–6 heulandite-group minerals is higher in calcium than clinoptilolites from drill holes C–I, Y–1, Y–7, and Y–8 and contains slightly less calcium than Y–2 intermediate heulandites (see fig. 9). The only other zeolite minerals found in drill core Y–6 are minor dachiardite and extensive mordenite.

Iron-rich hydrothermal minerals are very plentiful in the Y–6 drill core and include pyrite, marcasite, goethite, hematite, iron-rich chlorite, smectite (approximately 6 weight percent FeO), and siderite. Several carbonate minerals (calcite, Mn-calcite, Ca- and Fe-rhodochrosite, rhodochrosite, and siderite) contain varying amounts of manganese and iron.

Hydrothermal quartz and chalcedony are very abundant throughout most of the Y–6 drill core. Silica content of the analyzed Y–6 thermal water is about 244 mg/L, which indicates a maximum calculated temperature of about 194°C (table 1) rather than the 180.8°C measured during drilling. This difference in temperature may be significant in that quartz precipitates more readily at temperatures above 180°C and the potential for self-sealing is greater (White and others, 1971). Most of the fractures in the Y–6 drill core are partly to completely filled by hydrothermal silica and other minerals, and self-sealing appears to be a significant factor in interpreting the hydrothermal mineral sequence in this drill core.

White and others (1975) indicated that the low temperatures measured in the upper part of the Y–6 drill hole were probably due to cold meteoric water which percolated down through the covering of porous glacial sediments. The temperature of nearby hot springs ranges from 63° to 84°C, and hot springs near Lone Star Geyser, about 0.5 km east of Y–6, are mostly at or very near the surface boiling temperature for this elevation (Thompson and Yadav, 1979). The formation of hydrothermal potassium feldspar near the top of the Scaup Lake flow appears to be best explained by the loss of CO_2 and an increase in pH and the K/H ratio due to boiling of water (Keith and others, 1978b), probably during an earlier period of higher near-surface temperature.

White and others (1975) attributed the deeper Y–6 temperature profile, which is cooler than, but nearly parallel to, the reference boiling-point curve (fig. 2), to lateral movement of thermal water away from the main vertical channels and conductive heat loss. A decrease in temperature due to at least partial self-sealing is probably consistent with this hypothesis. Warmer temperatures in the past appear to be necessary to explain the abundance of open-space bladed calcite in the lower approximately 60 m of the drill core. Such deposits have been attributed to loss of CO_2 upon boiling of the geothermal water in other Yellowstone drill holes (Keith and others, 1978b; Keith and Muffler, 1978; Bargar and Beeson, 1981). Later crystalline to massive open-space fluorite deposits might also be partly due to decreasing solubility as a result of decreasing temperature of the geothermal water because of self-sealing of the main vertical channels and partly due to mixing of thermal water with cold meteoric water.

Homogenization temperatures were determined for 57 fluid inclusions in 4 samples from the lower one-half of the Y–6 drill core. The fluid inclusions appear to have formed over a wide temperature range (fig. 23). However, the minimum fluid inclusion temperatures plot very close to the measured temperature curve which suggests that this drill hole was significantly warmer in the past.

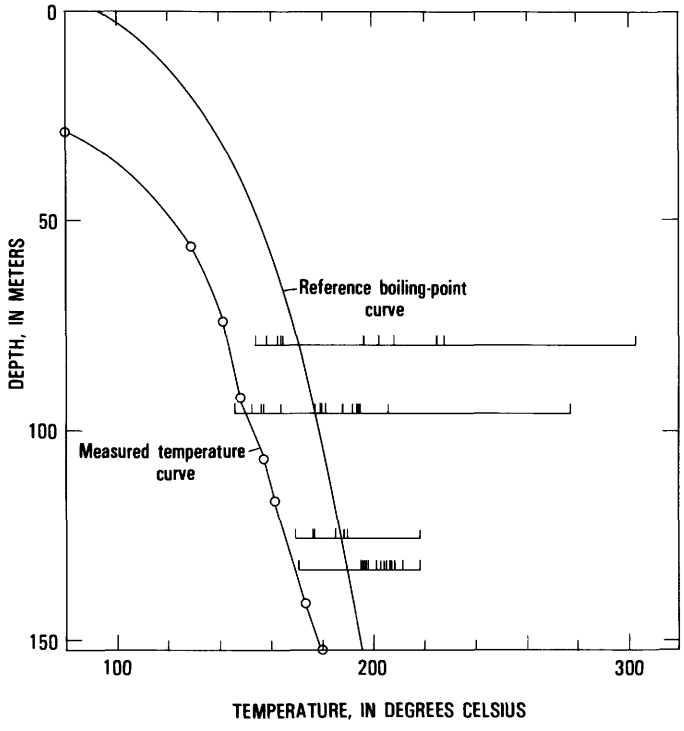

FIGURE 23.—Plot showing homogenization temperatures for fluid inclusions in fluorite (upper sample) and quartz (lower 3 samples) from Y–6 drill core.

REFERENCES CITED

Alberti, A., 1975, Sodium-rich dachiardite from Alpe de Siusi, Italy: contributions to Mineralogy and Petrology, v. 49, p. 63–66.

Alietti, A., 1972, Polymorphism and crystal-chemistry of heulandites and clinoptilolites: American Mineralogist, v. 57, p. 1448–1462.

Alietti, A., Brigatti, M. F., and Poppi, L., 1977, Natural Ca-rich clinoptilolites (heulandites of group 3): new data and review: Neues Jahrbuch fur Mineralogie Mn, v. 11, p. 494–501.

Allen, E. T., and Day, A. L., 1935, Hot springs of the Yellowstone National Park: Carnegie Institution of Washington Publication 466, 525 p.

Bargar, K. E., and Beeson, M. H., 1981, Hydrothermal alteration in research drill hole Y–2, Lower Geyser Basin, Yellowstone National Park Wyoming: American Mineralogist, v. 66, p. 473–490.

Bargar, K. E., Beeson, M. H., Fournier, R. O., and Muffler, L. J. P., 1973, Present-day deposition of lepidolite from thermal waters in Yellowstone National Park: American Mineralogist, v. 58, p. 901–904.

Bargar, K. E., Beeson, M. H., and Keith, T. E. C., 1981, Zeolites in Yellowstone National Park: Mineralogical Record, v. 12, p. 29–38.

Bargar, K. E., and Muffler, L. J. P., 1982, Hydrothermal alteration in research drill hole Y–11 from a vapor-dominated geothermal system at Mud Volcano, Yellowstone National Park, Wyoming: Wyoming Geological Association Annual Field Conference, 33d, Mammoth Hot Springs, Wyoming, Guidebook, p. 139–152.

Berry, L. G., Post, B., Weissman, S., McMurdie, H. F., and McClure, W. R., eds., 1974, Selected powder diffraction data for minerals: Philadelphia, Pennsylvania, Joint Committee on Powder Diffraction Standards, 833 p.

Boles, J. R., 1972, Composition, optical properties, cell dimensions, and thermal stability of some heulandite-group zeolites: American Mineralogist, v. 57, p. 1463–1493.

Bonardi, M., Roberts, A. C., and Sabina, A. P., 1981, Sodium-rich dachiardite from the Francon Quarry, Montreal Island, Quebec: Canadian Mineralogist, v. 19, p. 285–289.

Browne, P. R. L., 1970, Hydrothermal alteration as an aid in investigating geothermal fields: Geothermics, Special Issue 2, v. 2, pt. 1, p. 564–570.

———1978, Hydrothermal alteration in active geothermal fields: Annual Reviews in Earth and Planetary Sciences, v. 6, p. 229–250.

Browne, P. R. L., and Ellis, A. J., 1970, The Ohaki-Broadlands hydrothermal area, New Zealand: mineralogy and related geochemistry: American Journal of Science, v. 269, p. 97–131.

Cavarretta, G., Gianelli, G., and Puxeddu, M., 1980, Hydrothermal metamorphism in the Larderello Geothermal Field: Geothermics, v. 9, p. 297–314.

Christiansen, R. L., 1979, Cooling units and composite sheets in relation to caldera structure, *in* Chapin, C. E., and Elston, W. E., eds., Ash-flow tuffs: Geological Society of America Special Paper 180, p. 29–42.

Christiansen, R. L., and Blank, H. R., Jr., 1974, Geologic map of the Madison Junction quadrangle, Yellowstone National Park, Wyoming: U.S. Geological Survey Geologic Quadrangle Map GQ–1190, Scale 1:62,500.

Eaton, G. P., Christiansen, R. L., Iyer, H. M., Pitt, A. M., Mabey, D. R., Blank, H. R., Jr., Zietz, I., and Gettings, M. E., 1975, Magma beneath Yellowstone National Park: Science, v. 188, p. 787–796.

Fenner, C. N., 1936, Bore-hole investigations in Yellowstone Park: Journal of Geology, v. 44, p. 225–315.

Fournier, R. O., 1981, Application of water geochemistry to geothermal exploration and reservoir engineering, *in* Rybach, L., and Muffler, L. J. P., eds., Geothermal systems: Principles and case histories, New York, John Wiley and Sons, p. 109–143.

Fournier, R. O., and Truesdell, A. H., 1970, Chemical indicators of subsurface temperature applied to hot spring waters in Yellowstone National Park, Wyoming, U.S.A.: Geothermics, Special Issue 2, v. 2., pt. 1, p. 529–535.

Fournier, R. O., White, D. E., and Truesdell, A. H., 1976, Convective heat flow in Yellowstone National Park: Proceedings of the Second United Nations Symposium on Development and Use of Geothermal Resources, San Francisco, Calif., 20–29 May 1975, v. 1, Washington, D.C., U.S. Government Printing Office, p. 731–739.

Frondel, C., and Bauer, L. H., 1955, Kutnahorite: a manganese dolomite, $CaMn(CO_3)_2$: American Mineralogist, v. 40, p. 748–760.

Funiciello, R., Mariotti, G., Parotto, M., Preite-Martinez, M., Tecce, F., Toneatte, R., and Turi, B., 1979, Geology, mineralogy, and stable isotope geochemistry of the Cesano geothermal field (Sabatini Mtns. Volcanic system, Northern Latium, Italy): Geothermics, v. 8, p. 55–73.

Fytikas, M., Kouris, D., Marinelli, G., and Surcin, J., 1976, Preliminary geological data from the first two productive geothermal wells drilled at the island of Milos: International Congress on thermal waters, geothermal energy and vulcanism of the Mediterranean area, Athens, Proceedings, Geothermal Energy, v. 1, p. 511–515.

Goldsmith, J. R., and Graf., D. L., 1957, The system CaO-MnO-CO_2: Solid-solution and decomposition relations: Geochimica et Cosmochimica Acta, v. 11, p. 310–334.

Grim, R. E., 1968, Clay mineralogy: San Francisco, McGraw-Hill, 596 p.

Hawkins, D. B., 1974, Statistical analyses of the zeolites clinoptilolite and heulandite: Contributions to Mineralogy and Petrology, v. 45, p. 27–36.

Honda, S., and Muffler, L. J. P., 1970, Hydrothermal alteration in core from research drill hole Y-1, Upper Geyser Basin, Yellowstone National Park, Wyoming: American Mineralogist, v. 55, p. 1714–1737.

Hower, J., 1981, X-ray diffraction identification of mixed-layer clay minerals: Mineralogical Association of Canada Short Course, p. 39–59.

Huebner, J. S., 1969, Stability relations of rhodochrosite in the system manganese-carbon-oxygen: American Mineralogist, v. 54, p. 457–481.

Keith, T. E. C., Beeson, M. H., and White, D. E., 1978a, Hydrothermal minerals in U.S. Geological Survey research drill hole Y-13, Yellowstone National Park, Wyoming (Abs.): Geological Society of America Abstracts with Programs, v. 10, p. 432–433.

Keith, T. E. C., and Muffler, L. J. P., 1978, Minerals produced during cooling and hydrothermal alteration of ash flow tuff from Yellowstone drill hole Y-5: Journal of Volcanology and Geothermal Research, v. 3, p. 373–402.

Keith, T. E. C., White, D. E., and Beeson, M. H., 1978b, Hydrothermal alteration and self-sealing in Y-7 and Y-8 drill holes in northern part of Upper Geyser Basin, Yellowstone National Park, Wyoming: U.S. Geological Survey Professional Paper 1054–A, 26 p.

Kreiger, P., 1930, Notes on an X-ray diffraction study of the series calcite-rhodochrosite: American Mineralogist, v. 15, p. 23–29.

Lahodny-Sare, O., Dosen-Sver, D., and Keller, W. D., 1981, Scanning electron micrography of hydrothermally synthesized kaolin and parent materials during synthesis reactions: Tschermaks Mineralogische und Petrographische Mitteilungen, v. 28, p. 265–276.

Levison, W. G., 1916, Columnar manganocalcite from Franklin Furnace, N. J.: American Mineralogist, v. 1, p. 5.

McKibben, M. A., 1979, Ore minerals in the Salton Sea Geothermal System, Imperial Valley, California, U.S.A.: University of California, Riverside, unpublished M.S. thesis, 90 p.

Muffler, L. J. P., and Bargar, K. E., 1974, Hydrothermal alteration of rhyolitic ash-flow tuff in the vapor-dominated geothermal system at Mud Volcano, Yellowstone National Park, U.S.A. (Abs.): International Symposium on Water-Rock Interaction, Prague, Czechoslovakia, Abstract Volume, p. 52.

Mumpton, F. A., 1960, Clinoptilolite redefined: American Mineralogist, v. 45, p. 351–369.

Murata, K. J., and Larson, R. R., 1975, Diagenesis of Miocene siliceous shales, Temblor Range, California: U.S. Geological Survey Journal of Research, v. 3, p. 553–566.

Murata, K. J., and Norman, M. B., II, 1976, An index of crystallinity for quartz: American Journal of Science, v. 276, p. 1120–1130.

Omori, K., and Yamaoka, K., 1954, Towery manganocalcite from Hosokura mine, Miyagi Prefecture: Japanese Association of Mineralogists, Petrologists, and Economic Geologists Journal, no. 38-39, p. 81–86.

Pierce, K. L., Obradovich, J. D., and Friedman, I., 1976, Obsidian hydration dating and correlation of Bull Lake and Pinedale Glaciations near West Yellowstone, Montana: Geological Society of America Bulletin, v. 87, p. 703–710.

Reynolds, R. C., 1980, Interstratified clay minerals, *in* Brindley, G. W., and Brown, G., eds., Crystal structures of clay minerals and their X-ray identification: Mineralogical Society Monograph No. 5, p. 249–300.

Richardson, C. K., and Holland, H. D., 1979, Fluorite depostion in hydrothermal systems: Geochimica et Cosmochimica Acta, v. 43, p. 1327– 1335.

Rosenberg, P. E., 1963, Subsolidus relations in the system $CaCO_3$-$FeCO_3$: American Journal of Science, v. 26,p. 683–690.

———1967, Subsolidus relations in the system $CaCO_3$-$MgCO_3$-$FeCO_3$ between 350° and 550° C: American Mineralogist, v. 52, p. 787–796.

Sheridan, M. F., and Maisano, M. D., 1976, Zeolite and sheet silicate zonation in a Late-Tertiary geothermal basin near Hassayampa, central Arizona: Proceedings of the Second United Nations Symposium on the Development and Use of Geothermal Resources, San Francisco, Calif., 20–29 May, 1975, v. 1, Washington, D. C., U.S. Government Printing Office, p. 597–607.

Shibuya, G., and Harada, S., 1976, Mineralogical studies on kutnahorite and other carbonate minerals from the Hoei Mine, Oita Prefecture: Journal of the Mineralogical Society of Japan, v. 13, p. 1–25

Sigvaldson, G. E., and White, D. E., 1961, Hydrothermal alteration of rocks in two drill holes at Steamboat Springs, Washoe County, Nevada: U.S. Geological Survey Professional Paper 424–D, p. D116–D122.

———1962, Hydrothermal alteration in drill holes GS-5 and GS-7, Steamboat Springs, Nevada: U.S. Geological Survey Professional Paper 450–D, p. D113–D117.

Stauffer, R. E., 1982, Fluorapatite and fluorite solubility controls on geothermal waters in Yellowstone National Park: Geochimica et Cosmochimica Acta, v. 46, p. 465–474.

Stauffer, R. E., and Thompson, J. M., 1978, Phosphorous in hydrothermal waters of Yellowstone National Park, Wyoming: U.S. Geological Survey Journal of Research, v. 6, p. 755–763.

Steiner, A., 1977, The Wairakei geothermal area, North Island, New Zealand: Its subsurface geology and hydrothermal rock alteration: New Zealand Geological Survey Bulletin 90, 136 p.

Taylor, P., 1980, The stereochemistry of iron-sulfides—a structural rationale for the crystallization of some metastable phases from aqueous solution: American Mineralogist, v. 65, p. 1026–1030.

Thompson, J. M., Presser, T. S., Barnes, R. B., and Bird, D. B., 1975, Chemical analysis of the waters of Yellowstone National Park, Wyoming, from 1965 to 1973: U.S. Geological Survey Open-File Report 75–25, 59 p.

Thompson, J. M., and Yadav, S., 1979, Chemical analyses of waters from geysers, hot springs and pools in Yellowstone National Park, Wyoming, from 1974–1978: U.S. Geological Survey Open-File Report 79-704, 49 p.

Waldrop, H. A., 1975, Surficial geologic map of the Old Faithful quadrangle, Yellowstone National Park, Wyoming: U.S. Geological Survey Miscellaneous Geologic Investigations Map I–649, Scale 1:62,500.

White, D. E., 1955, Thermal springs and epithermal ore deposits, *in* Bateman, A. M., ed., Economic Geology, pt. 1: Urbana, Illinois, Economic Geology Publishing Company, p. 99–154.

———1978, Conductive heat flows in research drill holes in thermal areas of Yellowstone National Park, Wyoming: U.S. Geological Survey Journal of Research, v. 6, p. 765–774.

White, D. E., Fournier, R. O., Muffler, L. J. P., and Truesdell, A. H., 1975, Physical results of research drilling in thermal areas of Yellowstone National Park, Wyoming: U.S. Geological Survey Professional Paper 892, 70 p.

White, D. E., Muffler, L. J. P., and Truesdell, A. H., 1971, Vapor-dominated hydrothermal systems compared with hot-water systems: Economic Geology, v. 66, p. 75–97.

Wise, W. S., and Tschernich, R. W., 1978, Dachiardite-bearing assemblages in the Pacific Northwest, *in* Sand, L. B., and Mumpton, F. A., eds., Natural zeolites: occurrence, properties, use: New York, Pergamon Press, p. 105–111.

GPO 787-042/123